

Algebraic construction of adaptive coarse spaces for two-level schwarz preconditioners

Heinlein, Alexander; Smetana, Kathrin

DOI

[10.1137/23M1618193](https://doi.org/10.1137/23M1618193)

Publication date

2025

Document Version

Final published version

Published in

SIAM Journal on Scientific Computing

Citation (APA)

Heinlein, A., & Smetana, K. (2025). Algebraic construction of adaptive coarse spaces for two-level schwarz preconditioners. *SIAM Journal on Scientific Computing*, 47(2), A1170-A1197. <https://doi.org/10.1137/23M1618193>

Important note

To cite this publication, please use the final published version (if applicable). Please check the document version above.

Copyright

Other than for strictly personal use, it is not permitted to download, forward or distribute the text or part of it, without the consent of the author(s) and/or copyright holder(s), unless the work is under an open content license such as Creative Commons.

Takedown policy

Please contact us and provide details if you believe this document breaches copyrights. We will remove access to the work immediately and investigate your claim.

ALGEBRAIC CONSTRUCTION OF ADAPTIVE COARSE SPACES FOR TWO-LEVEL SCHWARZ PRECONDITIONERS*

ALEXANDER HEINLEIN[†] AND KATHRIN SMETANA[‡]

Abstract. Two-level domain decomposition preconditioners lead to fast convergence and scalability of iterative solvers. However, for highly heterogeneous problems with a rapidly varying coefficient function, the condition number of the preconditioned system generally depends on the contrast of the coefficient function. As a result, the convergence may deteriorate. Enhancing the coarse space by functions constructed from suitable local eigenvalue problems restores robust, contrast-independent convergence; these coarse spaces are often denoted as adaptive or spectral coarse spaces. However, these eigenvalue problems typically rely on nonalgebraic information such that the adaptive coarse spaces cannot be constructed from the fully assembled system matrix. In this paper, a novel algebraic adaptive coarse space which relies on the a -orthogonal decomposition of (local) finite element (FE) spaces into functions that solve the elliptic PDE with some trace and FE functions that are zero on the boundary is proposed. In particular, the basis is constructed from eigenmodes of two types of local eigenvalue problems associated with the edges of the domain decomposition. To approximate functions that solve the PDE locally, we employ a transfer eigenvalue problem which has originally been proposed for the construction of optimal local approximation spaces for multiscale methods. In addition, we make use of a Dirichlet eigenvalue problem that is a slight modification of the Neumann eigenvalue problem used in the adaptive generalized Dryja–Smith–Widlund (AGDSW) coarse space. Both eigenvalue problems rely solely on local Dirichlet matrices, which can be extracted from the fully assembled system matrix, allowing for an algebraic construction. By combining arguments from multiscale and domain decomposition methods, we derive a contrast-independent upper bound for the condition number. While we restrict ourselves here to a two-dimensional diffusion problem discretized by low-order FEs on regular meshes, the proposed framework is general, and we conjecture that the approach can be readily extended, for instance, to other elliptic problems, three dimensions, or, under mild assumptions, higher-order discretizations. The robustness of the method is confirmed numerically for a variety of heterogeneous coefficient distributions, including binary random distributions and a coefficient function constructed from the SPE10 benchmark. The results are comparable to those of the nonalgebraic AGDSW coarse space as well as for those cases where the convergence of the classical algebraic generalized Dryja–Smith–Widlund coarse space deteriorates. Moreover, the coarse space dimension is the same as or comparable to the AGDSW coarse space for all numerical experiments.

Key words. domain decomposition methods, multiscale methods, overlapping Schwarz preconditioner, adaptive coarse spaces

MSC codes. 65F08, 65F10, 65N55, 65N30, 68W10

DOI. 10.1137/23M1618193

1. Introduction. Domain decomposition methods (DDMs) are a popular class of methods that yield rapid convergence in the iterative solution of linear systems of equations arising from PDEs. In particular, if a suitable coarse level is used, then DDMs have proved to be scalable for a wide range of problems, which, for elliptic problems, can be shown theoretically by proving an upper bound for the condition number.

Unfortunately, in the presence of strong heterogeneities in certain problem parameters, the convergence of classical DDMs may deteriorate. For instance, for a

*Submitted to the journal's Numerical Algorithms for Scientific Computing section November 21, 2023; accepted for publication (in revised form) November 18, 2024; published electronically April 10, 2025.

<https://doi.org/10.1137/23M1618193>

[†]Delft Institute of Applied Mathematics, Delft University of Technology, 2628 CD Delft, The Netherlands (a.heinlein@tudelft.nl, <https://searhein.github.io/>).

[‡]Department of Mathematical Sciences, Stevens Institute of Technology, Hoboken, NJ 07030 USA (ksmetana@stevens.edu).

diffusion problem with a coefficient function that is varying rapidly on possibly several nonseparated scales, the condition number may depend on the contrast of the maximum and minimum values of the coefficient. One way to overcome this issue is by using adaptive coarse spaces, also known as spectral coarse spaces. These approaches are based on solving local generalized eigenvalue problems and selecting a number of eigenfunctions based on a user-chosen tolerance for the eigenvalues. The selected functions are used to construct coarse basis functions with local support. Due to the use of spectral information, these coarse spaces typically yield a provable upper bound of the condition number that is independent of the contrast and depends on the tolerance for the eigenvalues. Hence, adaptive coarse spaces yield robust convergence. A variety of adaptive coarse spaces has been introduced for nonoverlapping DDMs [43, 58, 37, 36, 10, 35, 47], most of which consider finite element (FE) tearing and interconnect–dual primal (FETI-DP) methods, balancing domain decomposition by constraints (BDDC) methods, and overlapping Schwarz methods [17, 15, 57, 25, 26, 27, 18, 38, 6].

Even though most of the approaches referenced above are provably robust, none is algebraic. This means that they cannot be constructed using only the fully assembled system matrix, requiring new assembly routines or even access to the mesh of the FE discretization. FETI-DP and BDDC methods are generally not algebraic since they require local Neumann matrices on the subdomains, which cannot be extracted from the system matrix. Schwarz methods can be constructed algebraically if the coarse space can be constructed algebraically. However, the adaptive coarse spaces mentioned above all require additional information for the definition of the eigenvalue problems, such as local Neumann matrices or geometric information.

In this paper, we propose, to the best of our knowledge for the first time, an interface-based adaptive coarse space for two-level overlapping Schwarz preconditioners that is robust and that can be constructed algebraically. Relying on the well-known a -orthogonal decomposition of local FE spaces into functions that solve the PDE numerically with a prescribed trace as a boundary condition and FE functions that are zero on the boundary, we propose in this paper building the adaptive coarse space from two local eigenvalue problems associated with each edge of the domain decomposition. To approximate functions that solve the PDE locally, we employ the transfer eigenvalue problem introduced in [54], which is known from the construction of optimal local approximation spaces [5, 54, 41, 51] for novel types of multiscale methods that allow full error control even for heterogeneous problems with nonseparated scales [5, 42, 41, 45, 46, 44, 54]. For the approximation of the functions with zero trace, we make use of a Dirichlet eigenvalue problem which is a slight modification of the Neumann eigenvalue problem used in the nonalgebraic adaptive generalized Dryja–Smith–Widlund (AGDSW) [26, 27, 38] coarse space. The adaptive coarse space is then built from energy-minimizing extensions of the eigenfunctions. Our new method is algebraic in the sense that both eigenvalue problems rely solely on local Dirichlet matrices, which can be extracted from the fully assembled system matrix. We show that using and combining arguments from these novel types of multiscale methods and DDMs allows deriving a contrast-independent upper bound for the condition number; the latter depends only mildly on the structure of the domain decomposition. For examples of how DDMs have been used to develop and analyze such novel types of multiscale methods, we refer the reader to [40, 39].

As most application codes generate a fully assembled system matrix, a robust DDM that solely uses this fully assembled matrix for the construction of the coarse space, as proposed in this paper, is clearly advantageous. In contrast to, for instance,

the AGDSW coarse space, which is not algebraic, the suggested approach has the disadvantage that it requires approximating two eigenvalue problems and is thus more costly. However, our numerical tests, including the ones in section 8, indicate that there is a chance that a coarse space only built from the eigenfunctions of the transfer eigenvalue problem might be robust. As for many other adaptive coarse spaces, our approach is based on solving eigenvalue problems on small subdomains; here, we consider a so-called oversampling domain which encloses the edge for which the coarse space is constructed. While a small oversampling domain (ideally just one layer of FEs around the edge) is computationally preferred for the construction of the coarse space, this may lead to unnecessarily large coarse spaces; see, for instance, the results in subsection 8.2. Finding the sweet spot here can be as challenging as it is in other adaptive coarse spaces which allow for varying the domain for the extensions, for instance, in AGDSW. One way to mitigate this issue is by tuning the tolerance in the construction of the coarse space, as discussed in section 8; however, this is also not straightforward to do for the just mentioned type of adaptive coarse spaces. Addressing these challenges is the subject of future work.

Even though we restrict ourselves to two-dimensional diffusion problems discretized by low-order FEs on regular meshes in this proof of concept, we conjecture that the proposed methodology can be easily extended to three dimensions, unstructured meshes, and other elliptic problems, such as linear elasticity and parabolic problems; cf. the extensions of the related AGDSW method [26, 27] and optimal local approximation spaces [54, 51, 52].

The adaptive coarse space proposed in this paper belongs to a class of adaptive coarse spaces which first partition the interface into nonoverlapping components and compute the eigenvalue problems on these components; cf. the spectral harmonically enriched multiscale [18], overlapping Schwarz–approximate component synthesis (OS-ACMS) [25], and AGDSW coarse spaces. All these approaches yield a minimum number of total degrees of freedom in all local generalized eigenvalue problems since no degree of freedom appears in more than one eigenvalue problem. Our new method is most closely related to the AGDSW method. Even though the AGDSW coarse space contains the generalized Dryja–Smith–Widlund (GDSW) coarse space [13, 14], which can be constructed algebraically, it is not algebraic since local Neumann matrices appear in the eigenvalue problems.

Algebraic coarse spaces for overlapping Schwarz methods have recently—and in parallel to the preparation of this manuscript—also been proposed by Gouarin and Spillane [21], Spillane [56], Al Daas and Grigori [2], Al Daas and Jolivet [3], and Al Daas, Jolivet, and Rees [4]. In all cases, the methods can be seen as extensions of the generalized eigenproblems in the overlaps (GenEO) [57] approach, where local eigenvalue problems in the overlaps or the overlapping subdomains of the Schwarz method are solved to compute the coarse space. In order to obtain algebraic coarse spaces, the authors mostly focus on general linear algebra arguments, such as matrix splittings and the Sherman–Morrison–Woodbury formula; see also [55, 1] for abstract descriptions of the GenEO framework. In contrast, our approach is based on a priori knowledge about the elliptic PDE.

Let us also briefly note that spectral information has also been used to improve the robustness of algebraic multigrid (AMG) methods [50], for instance, in the spectral element-based algebraic multigrid (ρ AMGe) method [11].

The paper is organized as follows. We propose adaptive coarse spaces for DDMs that can be constructed algebraically in section 5 and derive a bound for the condition number in section 6. Beforehand, we briefly introduce our heterogeneous diffusion

model problem in section 2 and review two-level overlapping Schwarz preconditioners in subsection 3.1 and adaptive coarse spaces in subsection 3.2. In particular, we also elaborate in section 4 on the challenges that arise when one wishes to construct adaptive coarse spaces without relying on local discrete variational problems with Neumann boundary conditions that would require new assembly routines on the local subdomains. Finally, we discuss the computational realization of the proposed method in section 7 and demonstrate its robustness numerically in section 8.

2. Problem setting. Let $\Omega \subset \mathbb{R}^2$ be a bounded domain with Lipschitz boundary and $\alpha \in L^\infty(\Omega)$ with $0 < \alpha_{\min} \leq \alpha \leq \alpha_{\max} < \infty$ be a highly heterogeneous coefficient function, possibly with high jumps. We consider the following variational problem:

$$(2.1) \quad \text{Find } u \in H_0^1(\Omega) : \quad a_\Omega(u, v) = \ell(v) \quad \forall v \in H_0^1(\Omega),$$

where $a_\Omega(u, v) := \int_\Omega \alpha(x) (\nabla u(x))^T \nabla v(x) dx$ and $\ell(v) := \int_\Omega \ell(x) v(x) dx,$

respectively, and $\ell \in L^2(\Omega)$. We equip $H_0^1(\Omega)$ with the energy norm $|u|_{a_\Omega} := (a_\Omega(u, u))^{1/2}$. Due to space limitations, we defer a discussion of the treatment of Neumann or mixed boundary conditions to a forthcoming paper.

Let τ_h be a quasi-uniform triangulation of Ω into triangles or quadrilaterals with element size h . To simplify the presentation, we assume that the triangulation resolves the coefficient function, i.e., that α is constant on each element. Then we introduce a conforming FE space $V_\Omega^0 \subset H_0^1(\Omega)$ of dimension N_Ω , where, for the sake of simplicity, we consider piecewise linear (P1) or bilinear (Q1) FE spaces. We obtain the following discrete variational problem:

$$(2.2) \quad \text{Find } u \in V_\Omega^0 : \quad a_\Omega(u, v) = f(v) \quad \forall v \in V_\Omega^0,$$

where $f(v) := \int_\Omega \ell(x) v(x) dx$ for $v \in V_\Omega^0$. The algebraic version of (2.2) then reads as follows:

$$(2.3) \quad \text{Find } \mathbf{u} \in \mathbb{R}^{N_\Omega} : \mathbf{A}\mathbf{u} = \mathbf{f}, \quad \text{where } \mathbf{A} \in \mathbb{R}^{N_\Omega \times N_\Omega}, \mathbf{f} \in \mathbb{R}^{N_\Omega}.$$

3. Adaptive coarse spaces for two-level overlapping Schwarz preconditioners.

3.1. Two-level overlapping Schwarz preconditioner. Let Ω be decomposed into nonoverlapping subdomains Ω_i with maximum diameter H such that $\bar{\Omega} = \bigcup_{i=1}^M \bar{\Omega}_i$, $\Omega_i \cap \Omega_j = \emptyset$ for $i \neq j$. We assume that the boundaries of the subdomains are Lipschitz continuous and do not intersect any element of τ_h . The domain decomposition interface is given as $\Gamma = \bigcup_{i \neq j} (\partial\Omega_i \cap \partial\Omega_j) \setminus \partial\Omega$. Then let $\{\Omega'_i\}_{i=1}^M$ be a corresponding overlapping decomposition of Ω with overlap $\delta \geq h$. We introduce associated conforming FE spaces $V_{\Omega'_i}^0 \subset H_0^1(\Omega'_i)$, $i = 1, \dots, M$, and introduce operators $R_{\Omega \rightarrow \Omega'_i} : V_\Omega^0 \rightarrow V_{\Omega'_i}^0$ that *restrict* FE functions in V_Ω^0 to $V_{\Omega'_i}^0$. The operators $E_{\Omega'_i \rightarrow \Omega} : V_{\Omega'_i}^0 \rightarrow V_\Omega^0$ *extend* FE functions in $V_{\Omega'_i}^0$ by zero to FE functions in V_Ω^0 accordingly. Note that the indices of the restriction and extension operators $R_{\Omega \rightarrow \Omega'_i}$ and $E_{\Omega'_i \rightarrow \Omega}$ here and henceforth show the domain of the respective FE spaces that the operators map from and to.¹ Moreover, in this paper, the indices at the bottom of the FE spaces show the domain

¹Very often, the operators $R_{\Omega \rightarrow \Omega'_i}$ and $E_{\Omega'_i \rightarrow \Omega}$ are denoted by R_i and R_i^T in the literature; see, e.g., [59]. As we will be needing also additional restriction and extension operators, e.g., for FE spaces on the edges or Γ , we indicate the domains of the associated FE spaces here.

that the space is associated with, and a 0 indicates that the functions in the FE space are zero on the boundary of the respective domain.

Next, we introduce local bilinear forms $a_{\Omega'_i} : V_{\Omega'_i}^0 \times V_{\Omega'_i}^0 \rightarrow \mathbb{R}$ and corresponding local stiffness matrices $\mathbf{A}_{\Omega'_i}$, $i = 1, \dots, M$. We use exact local solvers and thus obtain

$$(3.1) \quad a_{\Omega'_i}(u_i, v_i) = a_{\Omega}(E_{\Omega'_i \rightarrow \Omega} u_i, E_{\Omega'_i \rightarrow \Omega} v_i) \quad \forall u_i, v_i \in V_{\Omega'_i}^0, \quad \mathbf{A}_{\Omega'_i} = \mathbf{R}_{\Omega \rightarrow \Omega'_i} \mathbf{A} \mathbf{E}_{\Omega'_i \rightarrow \Omega}$$

for $i = 1, \dots, M$, where $\mathbf{R}_{\Omega \rightarrow \Omega'_i}$ and $\mathbf{E}_{\Omega'_i \rightarrow \Omega} = \mathbf{R}_{\Omega \rightarrow \Omega'_i}^T$ are the algebraic counterparts of $R_{\Omega \rightarrow \Omega'_i}$ and $E_{\Omega'_i \rightarrow \Omega}$, respectively; cf. [59]. Following, e.g., [59, 49], we introduce operators $\tilde{P}_i : V_{\Omega}^0 \rightarrow V_{\Omega'_i}^0$, defined as

$$(3.2) \quad a_{\Omega'_i}(\tilde{P}_i u, v_i) = a_{\Omega}(u, E_{\Omega'_i \rightarrow \Omega} v_i) \quad \text{for } v_i \in V_{\Omega'_i}^0, \quad i = 1, \dots, M.$$

We may then define projections

$$(3.3) \quad P_i = E_{\Omega'_i \rightarrow \Omega} \tilde{P}_i : V_{\Omega}^0 \rightarrow E_{\Omega'_i \rightarrow \Omega} V_{\Omega'_i}^0 \subset V_{\Omega}^0, \quad i = 1, \dots, M,$$

with algebraic counterparts $\mathbf{P}_i = \mathbf{E}_{\Omega'_i \rightarrow \Omega} \mathbf{A}_{\Omega'_i}^{-1} \mathbf{R}_{\Omega \rightarrow \Omega'_i} \mathbf{A}$, $i = 1, \dots, M$; see [59]. The additive Schwarz operator $P_{AS-1} := \sum_{i=1}^M P_i$ then reads in matrix form as

$$(3.4) \quad \mathbf{P}_{AS-1} := \sum_{i=1}^M \mathbf{E}_{\Omega'_i \rightarrow \Omega} \mathbf{A}_{\Omega'_i}^{-1} \mathbf{R}_{\Omega \rightarrow \Omega'_i} \mathbf{A} = \sum_{i=1}^M \mathbf{R}_{\Omega \rightarrow \Omega'_i}^T \mathbf{A}_{\Omega'_i}^{-1} \mathbf{R}_{\Omega \rightarrow \Omega'_i} \mathbf{A}.$$

This Schwarz operator is a preconditioned operator $\mathbf{M}_{AS-1}^{-1} \mathbf{A}$ consisting of the one-level Schwarz preconditioner $\mathbf{M}_{AS-1}^{-1} = \sum_{i=1}^M \mathbf{E}_{\Omega'_i \rightarrow \Omega} \mathbf{A}_{\Omega'_i}^{-1} \mathbf{R}_{\Omega \rightarrow \Omega'_i}$ and the system matrix \mathbf{A} . In this one-level Schwarz method, information is only exchanged between neighboring subdomains through the overlaps, and as a result, the convergence generally deteriorates for a large number of subdomains; see [49]. As a remedy, one may add a global coarse space $X_0 \subset V_{\Omega}^0$.² Correspondingly, we introduce an interpolation operator $E_0 : X_0 \rightarrow V_{\Omega}^0$, which expresses functions in X_0 in the FE basis of V_{Ω}^0 . The columns of the algebraic counterpart \mathbf{E}_0 therefore contain the FE coefficients of the basis functions of X_0 . Introducing the corresponding restriction operator $R_0 : V_{\Omega}^0 \rightarrow X_0$ and its algebraic counterpart $\mathbf{R}_0 = \mathbf{E}_0^T$, we can define $P_0 = E_0 \tilde{P}_0 : V_{\Omega}^0 \rightarrow E_0 X_0 \subset V_{\Omega}^0$. We define the operator \tilde{P}_0 analogously to (3.2), where

$$(3.5) \quad a_0(u_0, v_0) = a_{\Omega}(E_0 u_0, E_0 v_0) \quad \forall u_0, v_0 \in X_0, \quad \mathbf{A}_0 = \mathbf{R}_0 \mathbf{A} \mathbf{E}_0 = \mathbf{R}_0 \mathbf{A} \mathbf{R}_0^T;$$

this means that we also consider the case of an exact coarse solver. We then define the two-level Schwarz operator [59] $P_{AS-2} := \sum_{i=0}^M P_i$, and its algebraic counterpart takes the form

$$(3.6) \quad \mathbf{P}_{AS-2} = \mathbf{M}_{AS-2}^{-1} \mathbf{A} := \underbrace{\mathbf{E}_0 \mathbf{A}_0^{-1} \mathbf{R}_0 \mathbf{A}}_{\text{coarse level}} + \underbrace{\sum_{i=1}^M \mathbf{E}_{\Omega'_i \rightarrow \Omega} \mathbf{A}_{\Omega'_i}^{-1} \mathbf{R}_{\Omega \rightarrow \Omega'_i} \mathbf{A}}_{\text{first level}}.$$

Different choices of coarse spaces X_0 yield numerically scalable preconditioners, that is, a condition number bound which is independent of the number of subdomains. As a result, the convergence of iterative solvers, such as Krylov subspace methods,

²In many publications, the coarse space is denoted by V_0 . However, to avoid confusion with FE spaces including functions with zero trace, we denote the coarse space here by X_0 .

with such a two-level Schwarz preconditioner is independent of the number of subdomains as well. However, using a standard Lagrangian FE basis, for X_0 , we obtain the condition number bound

$$(3.7) \quad \kappa(\mathbf{P}_{AS-2}) = \kappa(\mathbf{M}_{AS-2}^{-1}\mathbf{A}) \leq C \max_{T \in \tau_H} \max_{x, y \in \omega_T} \left(\frac{\alpha(x)}{\alpha(y)} \right) \left(1 + \frac{H}{\delta} \right)$$

for our model problem (2.1); similar bounds hold for other classical (nonadaptive) coarse spaces. Here, τ_H is the coarse triangulation, which, in our case, coincides with the nonoverlapping domain decomposition $\{\Omega_i\}_{i=1, \dots, N}$. Moreover, ω_T corresponds to the union of all coarse mesh elements which touch a coarse mesh element T . Sharper variants of this estimate can be derived, but the dependence on the contrast of the coefficient function remains; see [22]. This means that the convergence of a Krylov subspace method preconditioned with this two-level Schwarz preconditioner might actually depend on the contrast of the coefficient function α , resulting in very high iteration counts; cf. also the results in section 8.

3.2. Adaptive coarse spaces. Figure 1 illustrates one of the reasons that the coefficient contrast may arise in the condition number bound. The energy

$$(3.8) \quad |\cdot|_{a, \Omega}^2 := a_{\Omega}(\cdot, \cdot)$$

of the function u plotted in Figure 1 (left) depends only on the minimum value α_{\min} of the coefficient function α but is independent of the maximum value α_{\max} , as its gradient is zero (hatched green) in the yellow region, where $\alpha = \alpha_{\max}$. If we interpolate the function with piecewise bilinear Lagrangian basis functions (see Figure 1 (right)), then the interpolant decays to zero within the yellow region (dotted red), and hence its energy clearly depends on α_{\max} . Therefore, in any energy estimate of the coarse interpolation, which is part of the proof of a condition number bound in the abstract Schwarz theory [59],

$$(3.9) \quad |u_0|_{a, \Omega}^2 \leq C |u|_{a, \Omega}^2,$$

the constant C has to depend on the contrast of α , $\alpha_{\max}/\alpha_{\min}$. Therefore, in order to obtain a robust condition number bound, the coefficient function has to be taken into account in the construction of the coarse space; as we will also observe in section 8, it is additionally necessary to add one coarse basis function for each high-coefficient component crossing the domain decomposition interface.

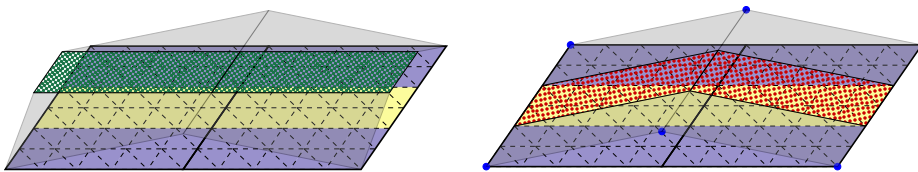


FIG. 1. For a heterogeneous coefficient function, a Lagrangian coarse interpolation (right; here, piecewise bilinear) of a low-energy function (left) may have a high energy: Let the yellow elements correspond to a high coefficient (α_{\max}) and the blue part to a low coefficient (α_{\min}). Since the function itself is constant (marked in hatched green) in the high-coefficient region but varying in the remaining part, the energy depends on α_{\min} but not on α_{\max} . The piecewise bilinear interpolation has a nonzero gradient everywhere such that the energy also depends on α_{\max} (marked in dotted red). In this case, the stability constant depends on the contrast of the coefficient function.

Adaptive coarse spaces account for variations in the coefficient functions by including eigenfunctions of local eigenvalue problems into the coarse space, which is why they are also denoted as *spectral coarse spaces*. The term *adaptive* stems from the fact that all eigenvalues below a certain tolerance tol can be included in the coarse space, resulting in a condition number bound of the form

$$(3.10) \quad \kappa(\mathbf{P}_{AS-2}) = \kappa(\mathbf{M}_{AS-2}^{-1}\mathbf{A}) \leq C \left(1 + \frac{1}{tol}\right),$$

where C is independent of the contrast of the coefficient function. Hence, the number of coarse basis functions does not have to be determined beforehand, but it can be chosen adaptively based on tol .

In this paper, we develop a new adaptive coarse space, consisting of basis functions which minimize the energy $|\cdot|_{a,\Omega_i}^2$ on each nonoverlapping subdomain given appropriately chosen Dirichlet data on the interface. Energy-minimizing functions are part of constructing a coarse space with a contrast-independent energy (3.9). Moreover, constructing the coarse basis by energy minimization is one of the key ingredients for algebraicity since it does not require the availability of a coarse triangulation. In particular, the energy-minimizing extension $v_i = H_{\partial\Omega_i \rightarrow \Omega_i}(v_{\partial\Omega_i})$ from $\partial\Omega_i$ to Ω_i for an FE function $v_{\partial\Omega_i}$ on $\partial\Omega_i$ is defined as follows: Given some boundary values $v_{\partial\Omega_i}$ on the interface, the corresponding extension $H_{\partial\Omega_i \rightarrow \Omega_i}(v_{\partial\Omega_i})$ solves

$$(3.11) \quad v_i = \arg \min_{v|_{\partial\Omega_i} = v_{\partial\Omega_i}} |v|_{a,\Omega_i}^2 \Leftrightarrow \begin{cases} a_{\Omega_i}(v_i, w_i) = 0 & \forall w_i \in V_{\Omega_i}^0, \\ v_i = v_{\partial\Omega_i} & \text{on } \partial\Omega_i. \end{cases}$$

An energy-minimizing extension $v = H_{\Gamma \rightarrow \Omega}(v_{\Gamma})$ extends interface values v_{Γ} into the interior of each subdomain, with zero Dirichlet boundary conditions on $\partial\Omega$. In matrix form, this corresponds to

$$(3.12) \quad \mathbf{v} = \begin{pmatrix} -\mathbf{A}_{II}^{-1}\mathbf{A}_{I\Gamma} \\ \mathbf{I}_{\Gamma} \end{pmatrix} \mathbf{v}_{\Gamma},$$

where we make use of the splitting of the rows and columns corresponding to interior (I) and interface (Γ) nodes $\mathbf{A} = \begin{pmatrix} \mathbf{A}_{II} & \mathbf{A}_{I\Gamma} \\ \mathbf{A}_{\Gamma I} & \mathbf{A}_{\Gamma\Gamma} \end{pmatrix}$ and \mathbf{I}_{Γ} corresponds to the identity matrix on Γ . Here, as usual, the Dirichlet boundary degrees of freedom are counted as interior. Due to the Dirichlet boundary conditions in \mathbf{A} , the boundary conditions are then enforced automatically. Note that $\mathbf{A}_{II} = \text{diag}(\mathbf{A}_{\Omega_i,II})$ is a block-diagonal matrix, where $\mathbf{A}_{\Omega_i,II}$ is the matrix corresponding to the interior degrees of freedom in Ω_i . Hence, in a parallel setting, \mathbf{A}_{II}^{-1} can be applied independently and concurrently for the subdomains. Moreover, we have that $|v|_{a,\Omega_i}^2 = a_{\Omega_i}(v, v) = \mathbf{v}^T \mathbf{A} \mathbf{v} = \mathbf{v}_{\Gamma}^T \mathbf{S} \mathbf{v}_{\Gamma}$, with the Schur complement $\mathbf{S} = \mathbf{A}_{\Gamma\Gamma} - \mathbf{A}_{\Gamma I} \mathbf{A}_{II}^{-1} \mathbf{A}_{I\Gamma}$.

Let us now discuss the general idea of adaptive coarse spaces which are based on an interface partition. To that end, let the interface Γ be partitioned into edges and vertices. In our discrete setting, we denote an edge as a set of connected interface FE nodes which belong to the same two subdomains; two nodes are denoted as connected if they belong to the same FE. A vertex is an interface FE node which belongs to more than two subdomains; cf. Figure 2. We then solve a generalized eigenvalue problem of the form

$$(3.13) \quad \text{find } \mathbf{v} \in \mathbb{R}^{N_e} \text{ such that } \mathbf{S}_e \mathbf{v} = \mu \mathbf{A}_{\tilde{e}\tilde{e}} \mathbf{v}$$

for each edge e , where N_e is the number of degrees of freedom of the interior of the edge e . Here, \mathbf{S}_e is a Schur complement corresponding to the two subdomains

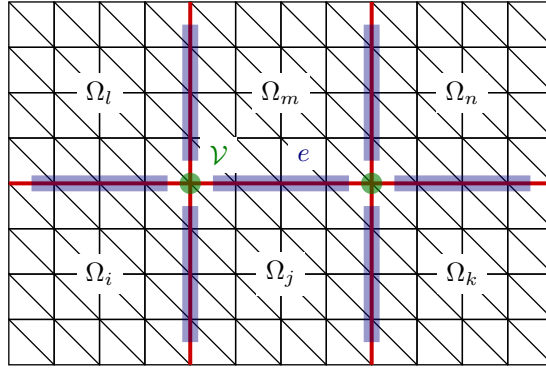


FIG. 2. Structured domain decomposition with six subdomains, seven edges (indicated by blue shaded boxes), and two vertices (indicated by green shaded circles). The vertex \mathcal{V} belongs to four subdomains, $\Omega_i, \Omega_j, \Omega_l, \Omega_m$, and the edge e is the set of FE nodes belonging to two subdomains, Ω_j, Ω_m .

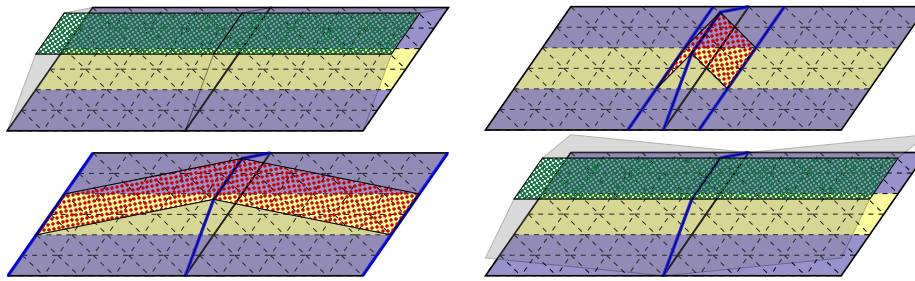


FIG. 3. For the same configuration as in Figure 1, we consider three different extensions of the edge values of a function (top left): the zero extension $E_{e \rightarrow \Omega_e}$ (top right), the harmonic extension with Dirichlet boundary data $H_{e \rightarrow \Omega_e}^{\partial \Omega_e}$ (bottom left), and a harmonic extension with Neumann boundary data $H_{e \rightarrow \Omega_e}$ (bottom right). The Dirichlet data of the extensions are marked in blue. In general, only the extension with Neumann boundary data has a guaranteed lower (or equal) energy compared to the original function; the energy of the other functions may even depend on the contrast.

Ω_i and Ω_j adjacent to e , and $\mathbf{A}_{\tilde{e}\tilde{e}}$ is the restriction of the global matrix \mathbf{A} to the degrees of freedom on the interior of the edge. As mentioned above, Schur complement matrices correspond to energy-minimizing extensions. In this eigenvalue problem, we consider such an extension from the edge e into the adjacent subdomains. The specific definition of \mathbf{S}_e may vary slightly for different interface-based adaptive coarse spaces, such as in the boundary conditions in the endpoints of the edge e . Moreover, $\mathbf{A}_{\tilde{e}\tilde{e}}$ can also be replaced by a scaled mass matrix or a lumped version of that.

To construct an adaptive coarse space, the eigenfunctions corresponding to eigenvalues below a user-chosen tolerance tol are selected and extended by zero onto the remaining interface. Then these functions are extended in an energy-minimizing way by $H_{\Gamma \rightarrow \Omega}$, resulting in the coarse basis functions.

As will be discussed in section 4 and visualized in Figure 3, eigenvalue problem (3.13) relates a low-energy extension (\mathbf{S}_e) and a high-energy extension ($\mathbf{A}_{\tilde{e}\tilde{e}}$). Therefore, the resulting coarse basis functions corresponding to low eigenvalues capture the critical components of the coefficient function, resulting in a condition number bound

of the form (3.10), which is independent of the contrast of the coefficient function; see, for instance, [18, 25, 26].

4. Motivation: Challenges and advantages of robust algebraic preconditioners and key new ideas. Despite the rapid development in adaptive coarse spaces, the development of algebraic variants, that is, variants that can be constructed based on the fully assembled system matrix \mathbf{A} , has been an open question for a longer time. For the practical applicability of a solver, this is, however, a desirable property. In particular, if the solver is algebraic, then it can be used in any FE implementation which provides the linear system of equations (2.3) as the solver input.

Let us briefly discuss the main challenge, which can be understood similarly to Figure 1. The left- and right-hand sides of the eigenvalue problem (3.13) correspond to energies of certain extensions of the edge values into the interior of the adjacent subdomains. In Figure 3 (top left), we see some function u with an energy $|u|_{a,\Omega}^2$ that does not depend on α_{\max} ; the gradient in the yellow region is zero (hatched green). In addition, three different extensions of the edge values of u are depicted: The extension on the top right is the extension by zero, and the corresponding energy clearly depends on α_{\max} (dotted red). The matrix on the right-hand side of (3.13) corresponds to this extension; that is, if $\mathbf{u}_{\tilde{e}}$ is the discrete vector with the interior edge values of u , then $\mathbf{u}_{\tilde{e}}^T \mathbf{A}_{\tilde{e}\tilde{e}} \mathbf{u}_{\tilde{e}}$ is the energy of the extension by zero (Figure 3 (top right)). This extension is algebraic since the matrix can be extracted from \mathbf{A} . The extension on the bottom right is the energy-minimizing extension of u_e with Neumann data on the boundary; of all functions with trace u_e , this function has the minimum energy, which is clearly smaller than or equal to the energy of u . Hence, the function satisfies an energy estimate of the form (3.9) with a constant C which does not depend on the contrast of α , $\frac{\alpha_{\max}}{\alpha_{\min}}$. This extension is one example of an extension that can be employed in \mathbf{S}_e on the left-hand side of (3.13).

Unfortunately, since this extension has Neumann boundary data, the corresponding matrix \mathbf{S}_e cannot be extracted algebraically from \mathbf{A} . An algebraic alternative to this extension would be the energy-minimizing extension with Dirichlet boundary data; cf. Figure 3 (bottom left). The Dirichlet submatrix corresponding to both subdomains adjacent to the edge e , which is required to compute this extension, can also be extracted from \mathbf{A} . However, the energy of this extension clearly depends on α_{\max} . Hence, using this algebraic extension in (3.13) would also result in a dependency on $\frac{\alpha_{\max}}{\alpha_{\min}}$. This short discussion explains why the Neumann matrix in (3.13) cannot be simply replaced by a Dirichlet matrix; this has also been discussed in [25]. It can be observed that, except for very recent approaches targeting algebraic adaptive coarse spaces, all early adaptive coarse spaces are based on eigenvalue problems which use Neumann matrices or information about the coefficient function and geometric information. Note that there have also been attempts to heuristically construct algebraic robust coarse spaces; cf., e.g., [25, 23, 29]. However, no theory has been proved for these approaches yet, and they might not be robust for arbitrary coefficient functions.

5. An algebraic and robust adaptive coarse space based on optimal local approximation spaces. In this section, we propose, to the best of our knowledge for the first time, an algebraic and robust adaptive interface-based coarse space. As we will only use Dirichlet matrices in the eigenvalue problems to obtain an algebraic method, we might miss the constant function in the edge space. However, it is well known in DDMs that a scalable coarse space has to be able to represent the null space of the global Neumann operator on each subdomain which does not touch the global Dirichlet boundary. Therefore, we start with the vertex and the edge spaces

$$(5.1) \quad X_{vert} = \text{span}\{H_{\Gamma \rightarrow \Omega}(E_{\mathcal{V} \rightarrow \Gamma}(1)) : \mathcal{V} \text{ vertex}\} \quad \text{and}$$

$$(5.2) \quad X_{const} = \text{span}\{H_{\Gamma \rightarrow \Omega}(E_{e \rightarrow \Gamma}(1)) : e \text{ edge}\},$$

respectively, containing the constant functions on the vertices and edges of the nonoverlapping domain decomposition $\{\Omega_i\}_{i=1,\dots,N}$. Here, $E_{\mathcal{V} \rightarrow \Gamma} : V_{\mathcal{V}} \rightarrow V_{\Gamma}^0$ and $E_{e \rightarrow \Gamma} : V_e^0 \rightarrow V_{\Gamma}^0$ extend the FE function by zero from the vertex \mathcal{V} or the edge e to the interface Γ , respectively. Recall that indices at the bottom of FE spaces show the domain that the space corresponds to, and a 0 indicates that the functions in the FE space are zero on the boundary of the respective domain. Then we enhance the edge space (5.2) by edge eigenfunctions of the *Dirichlet eigenvalue problem* introduced in subsection 5.1 and the *transfer eigenvalue problem* introduced in subsection 5.2.

Note that $X_{\text{GDSW}} = X_{vert} \oplus X_{const}$ corresponds to the classical GDSW coarse space. This space is also automatically included in the AGDSW adaptive coarse space. In particular, the constant edge function corresponds to the zero eigenvalue in the AGDSW edge eigenvalue problem due to full Neumann boundary data; hence, the function is always selected as a basis function.

5.1. A Dirichlet eigenvalue problem for the edges. As motivated in section 4, for each edge $e \subset \Gamma$, we consider a Dirichlet eigenvalue problem which is a slight modification of the Neumann eigenvalue problem (3.13) used in the AGDSW coarse spaces; cf. [26, 27]. First, we introduce for a fixed but arbitrary edge e a so-called oversampling domain Ω_e such that $\text{dist}(\partial\Omega_e, e) \geq v_e > 0$; see Figures SM2 in the supplementary material and 4 for illustrations of oversampling domains. In addition, we introduce $E_{e \rightarrow \Omega_e} : V_e^0 \rightarrow V_{\Omega_e}^0$, which assigns the coefficients of the FE functions on the edge e to the FE basis functions in Ω_e whose associated nodes lie on e and extends by zero on all other nodes in Ω_e ; see Figure 3 (top right) for an illustration.

We introduce the corresponding inner product $b_e : V_e^0 \times V_e^0 \rightarrow \mathbb{R}$ defined as

$$(5.3) \quad b_e(\chi, \zeta) := a_{\Omega_e}(E_{e \rightarrow \Omega_e}\chi, E_{e \rightarrow \Omega_e}\zeta) \quad \forall \chi, \zeta \in V_e^0.$$

Furthermore, we introduce the inner product $d_e : V_e^0 \times V_e^0 \rightarrow \mathbb{R}$ defined as

$$(5.4) \quad d_e(\chi, \zeta) := a_{\Omega_e}\left(H_{\dot{e} \rightarrow \Omega_e}^{\partial\Omega_e}(R_{e \rightarrow \dot{e}}\chi), H_{\dot{e} \rightarrow \Omega_e}^{\partial\Omega_e}(R_{e \rightarrow \dot{e}}\zeta)\right) \quad \forall \chi, \zeta \in V_e^0,$$

where \dot{e} denotes the discrete interior of the edge e and, algebraically, $R_{e \rightarrow \dot{e}}$ simply removes the degrees of freedom associated with the corners of the edge. Moreover, $H_{\dot{e} \rightarrow \Omega_e}^{\partial\Omega_e} : V_{\dot{e}} \rightarrow V_{\Omega_e}^0$ is defined as

$$a_{\Omega_e}(H_{\dot{e} \rightarrow \Omega_e}^{\partial\Omega_e}\chi, v) = 0 \quad \forall v \in V_{\Omega_e}^0, \quad H_{\dot{e} \rightarrow \Omega_e}^{\partial\Omega_e}\chi = 0 \text{ on } \partial\Omega_e, \quad H_{\dot{e} \rightarrow \Omega_e}^{\partial\Omega_e}\chi = \chi \text{ on } \dot{e};$$

hence, the upper index $\partial\Omega_e$ denotes that the harmonic extension has homogeneous Dirichlet boundary data on $\partial\Omega_e$ instead of Neumann boundary data; cf. the discussion in section 4. Finally, we denote by $\|\cdot\|_{b_e}$ and $\|\cdot\|_{d_e}$ the respective norms. We may then consider the following eigenvalue problem: Find $(\psi_e^{(i)}, \mu^{(i)}) \in (V_e^0, \mathbb{R}^+)$ such that

$$(5.5) \quad d_e(\psi_e^{(i)}, \chi) = \mu^{(i)} b_e(\psi_e^{(i)}, \chi) \quad \forall \chi \in V_e^0.$$

We select all $n_{dir,e}$ eigenfunctions corresponding to eigenvalues below a chosen tolerance tol_{dir} and define the space

$$(5.6) \quad X_{dir} := \text{span}\{H_{\Gamma \rightarrow \Omega}(E_{e \rightarrow \Gamma}\psi_e^{(i)}) : e \text{ edge}, \mu^{(i)} \leq tol_{dir}\}.$$

Here, $E_{e \rightarrow \Gamma} : V_e^0 \rightarrow V_\Gamma^0$ extends the FE function by zero from e to Γ , and $H_{\Gamma \rightarrow \Omega} : V_\Gamma^0 \rightarrow V_\Omega^0$ is the energy-minimizing extension from the interface into the interior of the subdomains as introduced in subsection 3.2. An eigenvalue problem similar to (5.5) has already been considered in [25]; however, alone, it is not generally robust.

We emphasize that none of the operators and matrices involved in (5.5) require any additional assembly and rely only on matrices that can be extracted from \mathbf{A} ; see section 7 for details. However, as can be seen in Table 1, choosing $X_0 = X_{vert} \oplus X_{const} \oplus X_{dir}$ does in general not yield a robust coarse space. To obtain a (provably) robust coarse space, we introduce a second eigenvalue problem.

5.2. Transfer eigenvalue problem. To obtain a robust coarse space, we exploit a well-known a -orthogonal decomposition of V_{Ω_e} ,³ namely, that every $u \in V_{\Omega_e}$ can be written as

$$(5.7) \quad u = u_{\Omega_e, ha} + u_{\Omega_e, ha}^\perp,$$

where $u_{\Omega_e, ha}^\perp \in V_{\Omega_e}^0$ and $u_{\Omega_e, ha}$ satisfies

$$(5.8) \quad a_{\Omega_e}(u_{\Omega_e, ha}, v) = 0 \quad \forall v \in V_{\Omega_e}^0 \quad \text{and} \quad u_{\Omega_e, ha}|_{\partial\Omega_e} = u|_{\partial\Omega_e}.$$

This means that it is an energy-minimizing extension; cf. (3.11). The decomposition (5.7) is a -orthogonal thanks to (5.8), and hence we have

$$(5.9) \quad a_{\Omega_e}(u_{\Omega_e, ha}, u_{\Omega_e, ha}^\perp) = 0 \quad \text{and} \quad |u|_{a, \Omega_e}^2 = |u_{\Omega_e, ha}|_{a, \Omega_e}^2 + |u_{\Omega_e, ha}^\perp|_{a, \Omega_e}^2.$$

In our approach, the eigenvalue problem from subsection 5.1 will serve to control the trace of functions in $V_{\Omega_e}^0$ on e . By introducing an eigenvalue problem on the space of functions that locally solve the PDE

$$(5.10) \quad V_{\Omega_e, ha} := \{w \in V_{\Omega_e} : a_{\Omega_e}(w, v) = 0 \quad \forall v \in V_{\Omega_e}^0\},$$

we can control the trace of functions in $V_{\Omega_e, ha}$ on e as well and therefore the traces of all functions in V_{Ω_e} on e . The fact that the decomposition is a -orthogonal and the right-hand side of (5.9) in particular will allow us to combine the contributions from both eigenvalue problems when deriving the bound for the condition number in section 6.

The eigenvalue problem we consider on the space of local solutions of the PDE $V_{\Omega_e, ha}$ has originally been suggested in a slightly different form in the context of multiscale and localized model order reduction methods in [54]. In that paper, it has been introduced to construct interface spaces that yield a provably optimally convergent static condensation approximation of the solution of the PDE. Similar to [54], we introduce a suitable inner product $(\cdot, \cdot)_{\partial\Omega_e} : V_{\partial\Omega_e} \times V_{\partial\Omega_e} \rightarrow \mathbb{R}$, where we require that the induced norm $\|\cdot\|_{\partial\Omega_e}$ satisfies

$$(5.11) \quad c_1 \|\zeta\|_{\partial\Omega_e} \leq \sqrt{\alpha_{min}} \|\zeta\|_{L^2(\partial\Omega_e)} \leq c_2 \|\zeta\|_{\partial\Omega_e} \quad \text{for all } \zeta \in V_{\partial\Omega_e},$$

with constants c_1 and c_2 that are independent of the mesh size and the coefficient α .

Remark 5.1 (discussion of inner product on $\partial\Omega_e$). Based on the proof in subsection 6.3, $a_{\Omega_e}(H_{\partial\Omega_e \rightarrow \Omega_e}(\cdot), H_{\partial\Omega_e \rightarrow \Omega_e}(\cdot))$ is a natural choice, as it leads to a very simple

³To simplify the notation, we assume here that $\partial\Omega_e \cap \partial\Omega = \emptyset$; otherwise, V_{Ω_e} has to be replaced by $V_{\Omega_e}^{\partial\Omega} := \{v \in V_{\Omega_e} : v = 0 \text{ on } \partial\Omega\}$ here and henceforth.

bound for the condition number. However, $a_{\Omega_e}(\cdot, \cdot)$ cannot be computed algebraically on V_{Ω_e} , as it requires the local Neumann matrices on Ω_e . Instead, we choose

$$(5.12) \quad (\chi, \zeta)_{\partial\Omega_e} = \alpha_{min} \frac{h}{N_{\partial\Omega_e}} (\chi, \zeta)_{l^2(\partial\Omega_e)},$$

which also satisfies (5.11) thanks to $\|\cdot\|_{L^2(\partial\Omega_e)}^2 \equiv \frac{h}{N_{\partial\Omega_e}} \|\cdot\|_{l^2(\partial\Omega_e)}^2$, where $N_{\partial\Omega_e}$ denotes the number of FE nodes on $\partial\Omega_e$. Note that α_{min} , h , and $N_{\partial\Omega_e}$ are only constant scaling factors which can be included into $(\cdot, \cdot)_{\partial\Omega_e}$ or the choice of a suitable tol_{tr} . In the algebraic setting, (estimates of) h and α_{min} may be provided by the user or have to be estimated within the algorithm; $N_{\partial\Omega_e}$ is known algebraically. Their estimates do not have to be very accurate, though, since constant factors do not affect eigenmodes or spectral gap size. For instance, h can be estimated roughly from dividing the diameter of Ω by the square root of the number nodes. For nonuniform triangulations, h would have to be replaced by the length $|\partial\Omega_e|$ in the equivalence of the L^2 - and l^2 -norms, and the availability of appropriate estimates of $|\partial\Omega_e|$ depends on the regularity and structure of the mesh. Alternatively, one may implement a strategy to detect the spectral gap in order to identify the eigenfunctions necessary for robustness; see, for instance, Figure SM1. For higher-order discretizations, potentially with p -refinement, an appropriate scaling of the inner product might be more involved. We remark that, even though the algebraic choice (5.12) yields a slightly more complicated condition number bound (see subsection 6.3), a numerical comparison in subsection SM2.2 shows that the coarse spaces corresponding to (5.12) and $a_{\Omega_e}(H_{\partial\Omega_e \rightarrow \Omega_e}(\cdot), H_{\partial\Omega_e \rightarrow \Omega_e}(\cdot))$ perform very similarly.

Next, as in [54], we introduce the transfer operator $\tilde{T}: V_{\partial\Omega_e} \rightarrow \{w|_e, w \in V_{\Omega_{e,ha}}\} := V_{\Omega_{e,ha}}^4$ defined as $\tilde{T}\zeta := (H_{\partial\Omega_e \rightarrow \Omega_e} \zeta)|_e$ for $\zeta \in V_{\partial\Omega_e}$, where the harmonic extension operator $H_{\partial\Omega_e \rightarrow \Omega_e}: V_{\partial\Omega_e} \rightarrow V_{\Omega_e}$ is defined as

$$a_{\Omega_e}(H_{\partial\Omega_e \rightarrow \Omega_e} \chi, v) = 0 \quad \forall v \in V_{\Omega_e}^0 \quad \text{and} \quad H_{\partial\Omega_e \rightarrow \Omega_e} \chi = \chi \quad \text{on} \quad \partial\Omega_e;$$

cf. subsection 3.2. However, since X_{vert} , introduced in (5.1), already accounts for the degrees of freedom in the vertices, we wish to only take into account the behavior of the functions in the interior of e . Therefore, we define the slightly modified transfer operator $T = (I - I_{\mathcal{V},e})\tilde{T}$, where $I_{\mathcal{V},e}$ denotes the restriction of $I_{\mathcal{V}}$ to e and $I_{\mathcal{V}}$ is the interpolation by the nodal functions in X_{vert} corresponding to the vertices. We then consider the following transfer eigenvalue problem: Find $(\phi_e^{(i)}, \lambda_i) \in (V_{\Omega_{e,ha}}, \mathbb{R}^+)$ such that

$$(5.13) \quad b_e(T(\phi_e^{(i)}|_{\partial\Omega_e}), T(w|_{\partial\Omega_e})) = \lambda^{(i)} (\phi_e^{(i)}|_{\partial\Omega_e}, w|_{\partial\Omega_e})_{\partial\Omega_e} \quad \forall w \in V_{\Omega_{e,ha}}.$$

We select the eigenfunctions corresponding to the $n_{tr,e}$ largest eigenvalues such that $\lambda^{(n_{tr,e})} > tol_{tr}$ and $\lambda^{(n_{tr,e}+1)} \leq tol_{tr}$ and introduce

$$(5.14) \quad \varphi_e^{(i)} = T(\phi_e^{(i)}|_{\partial\Omega_e}), \quad i = 1, \dots, \dim(V_{\Omega_{e,ha}}), \quad \text{and}$$

$$(5.15) \quad X_{tr} = \text{span}\{H_{\Gamma \rightarrow \Omega}(E_{e \rightarrow \Gamma}(\varphi_e^{(i)})) : e \text{ edge}, \lambda^{(i)} > tol_{tr}\}.$$

We highlight that thanks to (5.12), the calculation of the eigenfunctions of (5.13) only requires access to the global stiffness matrix \mathbf{A} ; for further details and the computational realization of (5.13), see section 7.

⁴Again, for $\partial\Omega_e \cap \partial\Omega \neq \emptyset$, one needs to replace $V_{\partial\Omega_e}$ by $V_{\partial\Omega_e}^{\partial\Omega} := \{v \in V_{\partial\Omega_e} : v = 0 \text{ on } \partial\Omega\}$.

Note that we may also perform a singular value decomposition (SVD) of the operator T , which reads as $T\zeta = \sum_i \sigma^{(i)} \hat{\varphi}^{(i)}(\chi^{(i)}, \zeta)_{\partial\Omega_e}$ for $\zeta \in V_{\partial\Omega_e}$ with orthonormal bases $\hat{\varphi}^{(i)} \in V_{\Omega_{e,ha}}^0 := \{(w|_e - I_{\mathcal{Y},e}(w|_e)), w \in V_{\Omega_{e,ha}}\}$, $\chi^{(i)} \in V_{\partial\Omega_e}$, and singular values $\sigma^{(i)} \in \mathbb{R}_0^+$. Then we have, up to numerical errors, $\sigma^{(i)} = \sqrt{\lambda^{(i)}}$ and $\text{span}\{\varphi_e^{(1)}, \dots, \varphi_e^{(n)}\} = \text{span}\{\hat{\varphi}^{(1)}, \dots, \hat{\varphi}^{(n)}\}$. We can thus infer from results of the optimality of the SVD that the space $\Lambda^n = \text{span}\{\varphi_e^{(1)}, \dots, \varphi_e^{(n)}\}$ minimizes $\|T - \Pi_{\Lambda^n} T\|$ among all n -dimensional subspaces of $V_{\Omega_{e,ha}}^0$ and hence optimally (in the sense of Kolmogorov) approximates the range of T and thus $V_{\Omega_{e,ha}}^0$; see also [5, 48, 54].

Remark 5.2. The direct extension to three-dimensional problems would require solving corresponding pairs of eigenvalue problems on the interface face; see also the extension of the AGDSW coarse space to three dimensions [26]. Alternatively, a different decomposition of the interface [27] or randomization [9] could be employed.

5.3. Complete definition of the adaptive coarse space. Finally, we define the complete adaptive coarse space X_0 as

$$(5.16) \quad X_0 = X_{\text{VCDT}} := X_{\text{vert}} \oplus X_{\text{const}} \oplus X_{\text{dir}} \oplus X_{\text{tr}},$$

where X_{vert} , X_{const} , X_{dir} , and X_{tr} were defined in (5.1), (5.2), (5.6), and (5.15), respectively.

6. Bound of the condition number. Since we use exact local and coarse solvers, (3.1) and (3.5), we obtain local stability with constant $\omega = 1$; cf. [59, Assumption 2.4] and, for the reader's convenience, Assumption SM1.1. Thanks to [59, Lemma 3.11 and follow-up discussion] and the proof of [16, Theorem 4.1], we obtain

$$(6.1) \quad \kappa(M_{AS-2}^{-1}A) \leq C_0^2(m+1),$$

where C_0^2 is the constant in the stable decomposition in Assumption 6.1 below and $m \in \mathbb{N}$ is an upper bound for the number of overlapping subdomains Ω'_i that any FE node in Ω can belong to. Hence, m only depends on the structure of the overlapping domain decomposition and is, for regular domain decompositions, bounded from above; also, for domain decompositions generated by mesh partitioners such as METIS [33], m is generally reasonably small. Therefore, it suffices to bound the constant C_0^2 in the stable decomposition to obtain a condition number bound.

Assumption 6.1 (stable decomposition [59, Assumption 2.2]). There exists a constant C_0 , such that every $u \in V_\Omega^0$ admits a decomposition

$$(6.2) \quad u = E_0 u_0 + \sum_{i=1}^M E_{\Omega'_i \rightarrow \Omega} u_i$$

$$(6.3) \quad \text{such that } \sum_{i=0}^M a_{\Omega'_i}(u_i, u_i) \leq C_0^2 a_\Omega(u, u).$$

6.1. Construction of the stable decomposition. One key novelty of the present manuscript which is a key ingredient for proving robustness lies in the specific definition of the coarse component u_0 . To that end, we define projection operators

$$(6.4) \quad \Pi_{e,dir} v := \sum_{i=1}^{n_{dir,e}} b_e(v, \psi_e^{(i)}) \psi_e^{(i)} \quad \forall v \in V_e^0 \quad \text{and}$$

$$(6.5) \quad \Pi_{e,tr} v := \sum_{i=1}^{n_{tr,e}} \frac{1}{\lambda^{(i)}} b_e(v, \varphi_e^{(i)}) \varphi_e^{(i)} \quad \forall v \in V_{\Omega_e,ha}^0,$$

where $n_{dir,e}$ and $n_{tr,e}$ denote the number of selected eigenfunctions from the eigenproblems (5.5) and (5.13), respectively. Note that for all $v \in V_{\Omega_e,ha}^0$ and $v = T(\tilde{v}|_{\partial\Omega_e})$, we have $\Pi_{e,tr} v = \sum_{i=1}^{n_{tr,e}} (\tilde{v}|_{\partial\Omega_e}, \phi^{(i)}|_{\partial\Omega_e})_{\partial\Omega_e} \varphi_e^{(i)}$, where $\phi^{(i)}$ is the i th eigenfunction of the transfer eigenvalue problem (5.13). Exploiting the latter and definition (5.14), $\varphi_e^{(i)} := T(\phi_e^{(i)}|_{\partial\Omega_e})$, yields the expression of $\Pi_{e,tr} v$ in (6.5). Moreover, we introduce the maps fitting the definitions of the coarse spaces X_{dir} and X_{tr} in (5.6) and (5.15):

$$\begin{aligned} \Pi_{dir} v &:= H_{\Gamma \rightarrow \Omega}(E_{e \rightarrow \Gamma}(\Pi_{e,dir} v)) \quad \forall v \in V_e^0 \quad \text{and} \\ \Pi_{tr} v &:= H_{\Gamma \rightarrow \Omega}(E_{e \rightarrow \Gamma}(\Pi_{e,tr} v)) \quad \forall v \in V_{\Omega_e,ha}^0. \end{aligned}$$

Definition of the coarse interpolation. As we will later use Poincaré's inequality, we have to include the constant function in our interpolation. This step will then introduce the minimum value of the coefficient function α_{\min} into the estimate, which is why we already included it on the right-hand side of the transfer eigenvalue problem; see (5.11). Our final condition number bound will still be robust since the maximum eigenvalue and, hence, the contrast will not appear. Similarly as in [54], we exploit that functions which are constant on Ω_e lie in $V_{\Omega_e,ha}$. We may thus write

$$(6.6) \quad u|_{\Omega_e} = \widehat{u_{\Omega_e,ha}} + c_u \mathbb{1}_{\Omega_e} + u_{\Omega_e,ha}^\perp, \quad \text{where} \quad \widehat{u_{\Omega_e,ha}} := u_{\Omega_e,ha} - c_u \mathbb{1}_{\Omega_e} \in V_{\Omega_e,ha}$$

and $c_u \in \mathbb{R}$ is zero when $\partial\Omega_e \cap \partial\Omega \neq \emptyset$ and will be selected later otherwise. We define the coarse interpolation

$$(6.7) \quad \begin{aligned} u_0 &:= H_{\Gamma \rightarrow \Omega}((I_{\mathcal{V}} u)|_{\Gamma}) + \sum_{e \in \Gamma} (u_{0,\Omega_e,ha} + u_{0,\Omega_e,ha}^\perp), \quad \text{where} \\ u_{0,\Omega_e,ha} &:= \Pi_{tr}(\widehat{u_{\Omega_e,ha}}|_e - I_{\mathcal{V},e} \widehat{u_{\Omega_e,ha}}|_e) + H_{\Gamma \rightarrow \Omega}(E_{e \rightarrow \Gamma}(c_u \mathbb{1}_e - I_{\mathcal{V},e} c_u \mathbb{1}_e)), \\ u_{0,\Omega_e,ha}^\perp &:= \Pi_{dir}(u_{\Omega_e,ha}^\perp|_e - I_{\mathcal{V},e} u_{\Omega_e,ha}^\perp|_e), \end{aligned}$$

where $I_{\mathcal{V}}$ is the interpolation by the nodal functions in X_{vert} corresponding to the vertices and $I_{\mathcal{V},e}$ is the restriction of this interpolation to the edge e . To simplify notations, we assume that u_0 is already expressed in the basis of V_{Ω}^0 .

Definition of the local components $u_i, i = 1, \dots, M$. As typical in the proof of condition number estimates for Schwarz methods, we define

$$(6.8) \quad u_i = R_{\Omega \rightarrow \Omega'_i} I^h(\theta_i(u - u_0)), \quad i = 1, \dots, M,$$

where $I^h(\theta_i(u - u_0)) \in V_{\Omega}^0$ denotes the interpolant of $\theta_i(u - u_0)$ and $\{\theta_i\}_{i=1}^M$ is a partition of unity corresponding to an overlapping decomposition $\{\tilde{\Omega}_i\}_{i=1}^M$ of Ω with overlap h ; hence, it is also a partition of unity on the overlapping domain decomposition $\{\Omega'_i\}_{i=1}^M$. In detail, we define $\theta_i(x_h) = 1$ in Ω_i , $\theta_i(x_h) = 1/m_{x_h}$ on Γ , and $\theta_i(x_h) = 0$ otherwise for all FE nodes x_h ; here, m_{x_h} denotes the number of subdomains that x_h belongs to. This definition ensures (6.2); see, for example, [59, section 3.6] for the same construction with a slightly different choice of the partition of unity.

6.2. Bound of the coarse-level and local contributions. The general structure of the proof follows earlier works, such as [18, 25, 26, 27]. We first prove estimates for the coarse and local components, as summarized in Lemma 6.2, and then combine them to the final estimate for C_0^2 in Proposition 6.7. Plugged into (6.1), we obtain the final condition number estimate. The main step in the proof is finding an upper bound for the term $|E_{e \rightarrow \Omega_e} [(u - u_0)|_e]|_{a, \Omega_e}^2$. This corresponds to upper bounds for $|w_{e_{ij}}(u - u_0)|_{a, \Omega_e}^2$ in OS-ACMS [25] or $|z_{\xi \rightarrow \Omega_\xi}(u - u_0)|_{a, \Omega_\xi}^2$ in AGDSW [26], respectively. The proof of this bound differs significantly for our new method and is the central novel contribution of the analysis in this manuscript and the topic of subsection 6.3. The remainder of the proof of the bound of the coarse-level and local contributions, as summarized in Lemma 6.2, is standard. It follows the earlier works listed above and can, for the reader's convenience, be found in subsection SM1.1.

LEMMA 6.2 (bound of the coarse-level and local contributions). *Let u_0 and u_i be defined as in (6.7) and (6.8), respectively, and let m_e denote the maximal number of edges e in a subdomain Ω_i . Then we have*

$$(6.9) \quad |u_0|_{a, \Omega}^2 \leq 2|u|_{a, \Omega}^2 + 2m_e \sum_{i=1}^M \sum_{e \subset \partial \Omega_i} |E_{e \rightarrow \Omega_e} [(u - u_0)|_e]|_{a, \Omega_e}^2,$$

$$(6.10) \quad \sum_{i=1}^M |u_i|_{a, \Omega_i}^2 \leq 18|u|_{a, \Omega}^2 + 15m_e \sum_{i=1}^M \sum_{e \subset \partial \Omega_i} |E_{e \rightarrow \Omega_e} [(u - u_0)|_e]|_{a, \Omega_e}^2,$$

where $E_{e \rightarrow \Omega_e}$ has been defined in the beginning of subsection 5.1.

6.3. Bound of the extension of $(u - u_0)|_e$. To complete the proof of the bound of the condition number, it thus remains to estimate the term $|E_{e \rightarrow \Omega_e} [(u - u_0)|_e]|_{a, \Omega_e}^2$. Different from other approaches, we decompose V_{Ω_e} in an a -orthogonal way and derive a bound for each part separately. The a -orthogonal decomposition allows combining both parts afterward. In particular, as already indicated in subsection 5.2 and more specifically in (5.7), we exploit that every $u \in V_{\Omega_e}$ can be written as

$$(6.11) \quad u = u_{\Omega_e, \text{ha}} + u_{\Omega_e, \text{ha}}^\perp,$$

where $u_{\Omega_e, \text{ha}}^\perp \in V_{\Omega_e}^0$ and $u_{\Omega_e, \text{ha}}$ satisfies

$$(6.12) \quad a_{\Omega_e}(u_{\Omega_e, \text{ha}}, v) = 0 \quad \forall v \in V_{\Omega_e}^0 \quad \text{and} \quad u_{\Omega_e, \text{ha}}|_{\partial \Omega_e} = u|_{\partial \Omega_e}.$$

Thanks to the definition of the coarse-level contribution (6.7), $u_{0, \Omega_e, \text{ha}}|_{e^*} = 0$ and $u_{0, \Omega_e, \text{ha}}^\perp|_{e^*} = 0$ for $e \neq e^*$, and the linearity of the interpolation operator $I_{\mathcal{V}}$, we get

$$(6.13) \quad |E_{e \rightarrow \Omega_e} [(u - u_0)|_e]|_{a, \Omega_e}^2 \leq 2 \left| E_{e \rightarrow \Omega_e} [(u_{\Omega_e, \text{ha}} - I_{\mathcal{V}} u_{\Omega_e, \text{ha}} - u_{0, \Omega_e, \text{ha}})|_e] \right|_{a, \Omega_e}^2 \\ + 2 \left| E_{e \rightarrow \Omega_e} [(u_{\Omega_e, \text{ha}}^\perp - I_{\mathcal{V}} u_{\Omega_e, \text{ha}}^\perp - u_{0, \Omega_e, \text{ha}}^\perp)|_e] \right|_{a, \Omega_e}^2.$$

Next, by exploiting the properties of the eigenvalue problems introduced in subsections 5.1 and 5.2, we will estimate the terms in (6.13) separately and combine the estimate at the end by exploiting a -orthogonality, that is,

$$(6.14) \quad |u|_{a, \Omega_e}^2 = |u_{\Omega_e, \text{ha}}|_{a, \Omega_e}^2 + |u_{\Omega_e, \text{ha}}^\perp|_{a, \Omega_e}^2.$$

Bound of the harmonic part. To estimate the terms containing the harmonic part of u , we will exploit that $\Lambda_n = \text{span}\{\varphi_e^{(1)}, \dots, \varphi_e^{(n)}\}$ minimizes $\|T - \Pi_{e, tr} T\|$ among all n -dimensional subspaces of $V_{\Omega_e, ha}^0$ (see the last paragraph of subsection 5.2 for the definition) and that for all $v \in V_{\Omega_e, ha} := \{w|_e, w \in V_{\Omega_e, ha}\}$, we have

$$(6.15) \quad \|(v|_e - I_{\mathcal{V}, e}(v|_e)) - \Pi_{e, tr}(v|_e - I_{\mathcal{V}, e}(v|_e))\|_{b_e} \leq \sqrt{tol_{tr}} \|v|_{\partial\Omega_e}\|_{\partial\Omega_e}.$$

This follows from the well-known fact that $\|T - \Pi_{e, tr} T\| = \sigma_{n_{tr, e} + 1}$, as Λ_n is the span of the first n left singular vectors of T ; cf. the Eckart–Young theorem, for instance, in [20] for the discrete setting; [48, Chapter 4, Theorem 2.2] for infinite-dimensional spaces; and [5, 54] for the derivation of error bounds for the local and global approximation error of optimally converging multiscale methods. We may show the following.

PROPOSITION 6.3 (bound of the harmonic part). *Let*

$$(6.16) \quad c_{t, e} := \sup_{v \in V_{\Omega_e, ha}} \frac{\|v|_{\partial\Omega_e}\|_{L^2(\partial\Omega_e)}}{\|v\|_{H^1(\Omega_e)}}, \quad c_{p, e} := \sup_{v \in V_{\Omega_e, ha}} \frac{\|v - \frac{c_{\Omega_e}}{|\Omega_e|} \int_{\Omega_e} v \mathbb{1}_{\Omega_e}\|_{L^2(\Omega_e)}}{\|\nabla v\|_{L^2(\Omega_e)}},$$

where $c_{\Omega_e} = 1$ if $\partial\Omega_e \cap \partial\Omega = \emptyset$ and 0 otherwise. Then we have

$$\left| E_{e \rightarrow \Omega_e} \left[(u_{\Omega_e, ha} - I_{\mathcal{V}} u_{\Omega_e, ha} - u_{0, \Omega_e, ha})|_e \right] \right|_{a, \Omega_e}^2 \leq \frac{c_{t, e}^2 tol_{tr} (1 + c_{p, e}^2)}{c_1^2} |u_{\Omega_e, ha}|_{a, \Omega_e}^2,$$

where c_1 depends on the choice of the bilinear form $(\cdot, \cdot)_{\partial\Omega_e}$ in (5.12); see (5.11).

Proof. By exploiting the definition of $u_{0, \Omega_e, ha}$ in (6.7), the restriction to the edge e , the linearity of the interpolation operators $I_{\mathcal{V}}$ and $I_{\mathcal{V}, e}$, the definition of $\widehat{u_{\Omega_e, ha}}$ in (6.6), and the definition of the inner product b_e in (5.3), we obtain

$$\begin{aligned} & \left| E_{e \rightarrow \Omega_e} \left[(u_{\Omega_e, ha} - I_{\mathcal{V}} u_{\Omega_e, ha} - u_{0, \Omega_e, ha})|_e \right] \right|_{a, \Omega_e}^2 \\ &= \left| E_{e \rightarrow \Omega_e} \left[(u_{\Omega_e, ha}|_e - I_{\mathcal{V}, e} u_{\Omega_e, ha}|_e) - \Pi_{e, tr}(\widehat{u_{\Omega_e, ha}}|_e - I_{\mathcal{V}, e} \widehat{u_{\Omega_e, ha}}|_e) \right. \right. \\ & \quad \left. \left. - (c_u \mathbb{1}_e - I_{\mathcal{V}, e} c_u \mathbb{1}_e) \right] \right|_{a, \Omega_e}^2 \\ &= \left\| (\widehat{u_{\Omega_e, ha}}|_e - I_{\mathcal{V}, e} \widehat{u_{\Omega_e, ha}}|_e) - \Pi_{e, tr}(\widehat{u_{\Omega_e, ha}}|_e - I_{\mathcal{V}, e} \widehat{u_{\Omega_e, ha}}|_e) \right\|_{b_e}^2. \end{aligned}$$

As $\widehat{u_{\Omega_e, ha}}|_e$ is in $V_{\Omega_e, ha} = \{w|_e, w \in V_{\Omega_e, ha}\}$, we may then invoke (6.15) and obtain

$$(6.17) \quad \left| E_{e \rightarrow \Omega_e} \left[(u_{\Omega_e, ha} - I_{\mathcal{V}} u_{\Omega_e, ha} - u_{0, \Omega_e, ha})|_e \right] \right|_{a, \Omega_e}^2 \leq tol_{tr} \|\widehat{u_{\Omega_e, ha}}|_{\partial\Omega_e}\|_{\partial\Omega_e}^2.$$

To conclude the estimate of the harmonic part of the function, we exploit (5.11) and choose c_u in $\widehat{u_{\Omega_e, ha}} := u_{\Omega_e, ha} - c_u \mathbb{1}_{\Omega_e}$, as $c_u = (1/|\Omega_e|) \int_{\Omega_e} u_{\Omega_e, ha}$ if $\partial\Omega_e \cap \partial\Omega = \emptyset$ and $c_u = 0$ otherwise. Now we apply the trace theorem and the Poincaré inequality:

$$(6.18) \quad \begin{aligned} & \left| E_{e \rightarrow \Omega_e} \left[(u_{\Omega_e, ha} - I_{\mathcal{V}} u_{\Omega_e, ha} - u_{0, \Omega_e, ha})|_e \right] \right|_{a, \Omega_e}^2 \\ & \leq tol_{tr} \frac{\alpha_{min}}{c_1^2} \|\widehat{u_{\Omega_e, ha}}|_{\partial\Omega_e}\|_{L^2(\partial\Omega_e)}^2 \\ & \leq tol_{tr} \frac{c_{t, e}^2 \alpha_{min}}{c_1^2} (\|\widehat{u_{\Omega_e, ha}}\|_{L^2(\Omega_e)}^2 + \|\nabla \widehat{u_{\Omega_e, ha}}\|_{L^2(\Omega_e)}^2) \\ & \leq tol_{tr} \frac{c_{t, e}^2 \alpha_{min}}{c_1^2} (1 + c_{p, e}^2) \|\nabla u_{\Omega_e, ha}\|_{L^2(\Omega_e)}^2 \leq \frac{c_{t, e}^2 tol_{tr}}{c_1^2} (1 + c_{p, e}^2) |u_{\Omega_e, ha}|_{a, \Omega_e}^2. \quad \square \end{aligned}$$

Remark 6.4. Taking the supremum in (6.16) over V_{Ω_e} shows that $c_{t, e}$ and $c_{p, e}$ do not depend on the contrast of the coefficient function.

Bound of the perpendicular part. By exploiting that the eigenfunctions $\psi_e^{(i)}$, $i = 1, \dots, \dim(V_e^0)$, of (5.5) span V_e^0 and that we select all $n_{dir,e}$ eigenfunctions corresponding to eigenvalues below a chosen tolerance tol_{dir} to define the space X_{dir} , we obtain by standard spectral arguments for adaptive coarse spaces that

(6.19)

$$\|v\|_{d_e}^2 = \|\Pi_{e,dir}v\|_{d_e}^2 + \|v - \Pi_{e,dir}v\|_{d_e}^2, \quad \|v - \Pi_{e,dir}v\|_{b_e}^2 \leq \frac{1}{tol_{dir}} \|v - \Pi_{e,dir}v\|_{d_e}^2$$

for each $v \in V_e^0$; cf., e.g., [37, 57, 25]. Using (6.19), we can show the following result.

PROPOSITION 6.5 (bound of the perpendicular part). *We have*

$$(6.20) \quad \left| E_{e \rightarrow \Omega_e} \left[\left(u_{\bar{\Omega}_{e,ha}}^\perp - I_{\mathcal{V}} u_{\bar{\Omega}_{e,ha}}^\perp - u_{0,\Omega_e,ha}^\perp \right) |e \right] \right|_{a,\Omega_e}^2 \leq \frac{1}{tol_{dir}} |u_{\bar{\Omega}_{e,ha}}^\perp|_{a,\Omega_e}^2.$$

Proof. By exploiting the definition of $u_{\bar{\Omega}_{e,ha}}^\perp$ in (6.7), the restriction to the edge e , the linearity of the interpolation operators $I_{\mathcal{V}}$ and $I_{\mathcal{V},e}$, the definition of the inner product b_e in (5.3), and (6.19), we obtain

$$\begin{aligned} & \left| E_{e \rightarrow \Omega_e} \left[\left(u_{\bar{\Omega}_{e,ha}}^\perp - I_{\mathcal{V}} u_{\bar{\Omega}_{e,ha}}^\perp - u_{0,\Omega_e,ha}^\perp \right) |e \right] \right|_{a,\Omega_e}^2 \\ &= \left| E_{e \rightarrow \Omega_e} \left[\left((u_{\bar{\Omega}_{e,ha}}^\perp |e - I_{\mathcal{V},e} u_{\bar{\Omega}_{e,ha}}^\perp |e) - \Pi_{e,dir} (u_{\bar{\Omega}_{e,ha}}^\perp |e - I_{\mathcal{V},e} u_{\bar{\Omega}_{e,ha}}^\perp |e) \right) \right] \right|_{a,\Omega_e}^2 \\ &= \left\| (u_{\bar{\Omega}_{e,ha}}^\perp |e - I_{\mathcal{V},e} u_{\bar{\Omega}_{e,ha}}^\perp |e) - \Pi_{e,dir} (u_{\bar{\Omega}_{e,ha}}^\perp |e - I_{\mathcal{V},e} u_{\bar{\Omega}_{e,ha}}^\perp |e) \right\|_{b_e}^2 \\ &\stackrel{(6.19)}{\leq} \frac{1}{tol_{dir}} \|u_{\bar{\Omega}_{e,ha}}^\perp |e - I_{\mathcal{V},e} u_{\bar{\Omega}_{e,ha}}^\perp |e\|_{d_e}^2. \end{aligned}$$

A close inspection of the definition of the inner product d_e in (5.4) reveals that, as we have $R_{e \rightarrow \hat{e}}(u_{\bar{\Omega}_{e,ha}}^\perp |e - I_{\mathcal{V},e} u_{\bar{\Omega}_{e,ha}}^\perp |e) = R_{e \rightarrow \hat{e}}(u_{\bar{\Omega}_{e,ha}}^\perp |e)$, there holds that

$$\|u_{\bar{\Omega}_{e,ha}}^\perp |e - I_{\mathcal{V},e} u_{\bar{\Omega}_{e,ha}}^\perp |e\|_{d_e}^2 = a_{\Omega_e} (H_{\hat{e} \rightarrow \Omega_e}^{\partial \Omega_e} R_{e \rightarrow \hat{e}}(u_{\bar{\Omega}_{e,ha}}^\perp |e), H_{\hat{e} \rightarrow \Omega_e}^{\partial \Omega_e} R_{e \rightarrow \hat{e}}(u_{\bar{\Omega}_{e,ha}}^\perp |e)).$$

As $u_{\bar{\Omega}_{e,ha}}^\perp \in V_{\Omega_e}^0$ and the discrete harmonic extension $H_{\hat{e} \rightarrow \Omega_e}^{\partial \Omega_e} R_{e \rightarrow \hat{e}}(u_{\bar{\Omega}_{e,ha}}^\perp |e)$ minimizes the $|\cdot|_{a,\Omega_e}$ -norm among all functions in $V_{\Omega_e}^0$ that equal $u_{\bar{\Omega}_{e,ha}}^\perp$ on \hat{e} , we conclude that

$$\|u_{\bar{\Omega}_{e,ha}}^\perp |e - I_{\mathcal{V},e} u_{\bar{\Omega}_{e,ha}}^\perp |e\|_{d_e}^2 \leq |u_{\bar{\Omega}_{e,ha}}^\perp |e|_{a,\Omega_e}^2. \quad \square$$

Combining the bounds of the harmonic and perpendicular parts. By invoking the stability result (6.14) and exploiting the estimate (6.13) and Propositions 6.3 and 6.5, we obtain the following result.

COROLLARY 6.6. *We have*

$$|E_{e \rightarrow \Omega_e} [(u - u_0)|e]|_{a,\Omega_e}^2 \leq 2 \max \left\{ \frac{c_{t,e}^2 tol_{tr} (1 + c_{p,e}^2)}{c_1^2}, \frac{1}{tol_{dir}} \right\} |u|_{a,\Omega_e}^2.$$

6.4. Complete bound of the condition number. By combining Lemma 6.2 and Corollary 6.6, we obtain the following bound for the condition number.

PROPOSITION 6.7. Let u_0 and u_i , $i = 1, \dots, M$, be defined as in (6.7) and (6.8), respectively. Let further m_e denote the maximal number of edges e in a subdomain Ω_i , $\nu := \max_{e \in \Gamma} \{\text{number of subdomains } \Omega_i \text{ that satisfy } \Omega_i \cap \hat{e} \neq \emptyset\}$, $\tilde{\omega} = \max_{i=1, \dots, M} \{\text{number of } \Omega_e \text{ such that } \Omega_e \cap \Omega_i \neq \emptyset\}$, $c_t := \max_{e \in \Gamma} c_{t,e}$, and $c_p := \max_{e \in \Gamma} c_{p,e}$, where $c_{t,e}$ and $c_{p,e}$ have been defined in (6.16). Then the condition number can be bounded as $\kappa(\mathbf{M}_{AS-2}^{-1} \mathbf{A}) \leq C_0^2 (m+1)$ with

$$(6.21) \quad C_0^2 := \left(20 + 34m_e \nu \tilde{\omega} \max \left\{ \frac{c_t^2 \text{tol}_{tr} (1 + c_p^2)}{c_1^2}, \frac{1}{\text{tol}_{dir}} \right\} \right)$$

in the stable decomposition in Assumption 6.1.

Remark 6.8. The bound in Proposition 6.7 is only mildly affected by the structure of the domain decomposition via the Poincaré constant $c_{p,e}$. As can be seen in (6.18), the latter is defined on the oversampling domain Ω_e , and it depends on both the size and the regularity of Ω_e ; see, for example, [13, Lemma 2.2]. We assume that Ω_e is relatively small in size, neither very thin nor with a boundary featuring very pointed parts, and we therefore conjecture that the Poincaré constant will only have a minor effect on the bound.

Remark 6.9. Compared with numerical results in section 8, the condition number bound (6.21) is pessimistic. However, it correctly states the scalability and the robustness with respect to coefficient jumps of the coarse space. This is similar to the bounds in many other adaptive coarse spaces; see, for instance, [18, 25].

Remark 6.10. The bilinear form in Remark 5.1 enabling the algebraic construction of our coarse space depends on the parameters α_{min} , h , and $N_{\partial\Omega_e}$, which are constant under our assumptions. Whereas $N_{\partial\Omega_e}$ is known algebraically, α_{min} and h may be provided by the user or have to be estimated. Their estimate does not have to be very accurate since constant factors do not affect eigenmodes or spectral gap size.

7. Computational realization. In this section, we briefly discuss the algorithmic steps for the algebraic construction of the different components of the two-level Schwarz preconditioner (3.6) with the adaptive coarse space X_0 (5.16). As $X_{GDSW} = X_{vert} \oplus X_{const} \subset X_0$ (cf. the discussion at the beginning of section 5), many algorithmic building blocks are the same as in the standard GDSW preconditioner. We thus mainly focus here on the Dirichlet and transfer eigenvalue problems and refer the reader to [31, 24] for details on the algebraic construction of GDSW preconditioners.

The main algorithmic components of the two-level preconditioner (3.6). Since $\mathbf{E}_{\Omega'_i \rightarrow \Omega} = \mathbf{R}_{\Omega \rightarrow \Omega'_i}^T$ and $\mathbf{E}_0 = \mathbf{R}_0^T$ and thus $\mathbf{A}_{\Omega'_i} = \mathbf{R}_{\Omega \rightarrow \Omega'_i} \mathbf{A} \mathbf{R}_{\Omega \rightarrow \Omega'_i}^T$ and $\mathbf{A}_0 = \mathbf{R}_0 \mathbf{A} \mathbf{R}_0^T$, it is sufficient to construct the operators $\mathbf{R}_{\Omega \rightarrow \Omega'_i}$ for $i = 1, \dots, M$ and \mathbf{R}_0 .

Nonoverlapping domain decomposition. Let us assume that a nonoverlapping domain decomposition $\bar{\Omega} = \cup_i \bar{\Omega}_i$ is already given or can be obtained from the sparsity pattern of the matrix \mathbf{A} using a graph partitioner, such as METIS [34].

Restriction operators on the first level. For the first level, the operators $\mathbf{R}_{\Omega \rightarrow \Omega'_i}$ extract the subvector corresponding to Ω'_i when applied to a global FE vector. Similarly, $\mathbf{A}_{\Omega'_i} = \mathbf{R}_{\Omega \rightarrow \Omega'_i} \mathbf{A} \mathbf{R}_{\Omega \rightarrow \Omega'_i}^T$ can be obtained by extracting the submatrix corresponding to Ω'_i from \mathbf{A} . Hence, the $\mathbf{R}_{\Omega \rightarrow \Omega'_i}$ never have to be set up explicitly.

To define the action of the operator $\mathbf{R}_{\Omega \rightarrow \Omega'_i}$, it is sufficient to identify the index set of the subdomain Ω'_i . Starting from the nonoverlapping subdomain Ω_i , the overlapping subdomain can be constructed recursively by adding layers of FE nodes.

This can, again, be performed based on the sparsity pattern of \mathbf{A} , making use of the fact that two FE nodes share a nonzero off-diagonal coefficient in \mathbf{A} if they are adjacent.

Computation of the coarse basis functions. The coarse basis functions in terms of the FE basis functions are stored in the columns of \mathbf{E}_0 . If we have computed the interface values $\mathbf{E}_{0,\Gamma}$ of the coarse basis functions, the interior values are then computed as energy-minimizing extensions from the interface to the interior of the subdomains $\mathbf{E}_{0,I} = -\mathbf{A}_{II}^{-1} \mathbf{A}_{I\Gamma} \mathbf{E}_{0,\Gamma}$; cf. (3.11) and (3.12) and the discussion in subsection 3.2.

The steps above require a partition into interior and interface nodes. Based on their multiplicity in the nonoverlapping domain decomposition, the nodes can be algebraically categorized as interior (multiplicity 1), edge (multiplicity 2), or vertex (multiplicity > 2).

Remark 7.1. As mentioned in section 5, we begin the construction of $\mathbf{E}_{0,\Gamma}$ with a basis for the vertex and edge spaces X_{vert} and X_{const} , respectively, spanning the null space. For a nodal basis, we can simply restrict the vector $\mathbf{1}$ with only 1 entries to the vertices and edges. If the basis is not nodal, for instance, for high-order discretizations, then we assume that a basis of the null space is provided as a user input. This is a typical requirement for nonstandard null spaces in algebraic preconditioning packages, such as the AMG and DD packages MueLu [7] and FROSch [30] from Trilinos [32].

7.1. Algebraic construction of coarse edge functions from Dirichlet and transfer eigenvalue problem.

Construction of Ω_e . Both eigenvalue problems require the oversampling domain Ω_e corresponding to each edge e . It can be constructed similarly to the overlapping subdomains: We start with the FE nodes of the interior of the edge e and extend the set recursively by layer of FE nodes using the sparsity pattern of \mathbf{A} ; cf. Figure 4.

Dirichlet eigenvalue problem (5.5). The Dirichlet eigenvalue problems can be written as follows: Find $(\mathbf{v}, \mu) \in \mathbb{R}^{N_{\dot{e}}} \times \mathbb{R}^+$ such that

$$\mathbf{S}_e \mathbf{v} = \mu \mathbf{A}_{\dot{e}\dot{e}} \mathbf{v}$$

with matrices \mathbf{S}_e and $\mathbf{A}_{\dot{e}\dot{e}}$; see also (3.13). The latter can easily be extracted from \mathbf{A} ; it is the submatrix corresponding to the interior edge nodes. The Schur complement on the left-hand side is given by $\mathbf{S}_e = \mathbf{A}_{\dot{e}\dot{e}} - \mathbf{A}_{\dot{e}\tilde{R}} \mathbf{A}_{\tilde{R}\tilde{R}}^{-1} \mathbf{A}_{\tilde{R}\dot{e}}$, where the index set \tilde{R} corresponds to the interior nodes of Ω_e except for the interior nodes of e . As $\mathbf{A}_{\dot{e}\dot{e}}$, the matrices $\mathbf{A}_{\dot{e}\tilde{R}}$, $\mathbf{A}_{\tilde{R}\tilde{R}}$, and $\mathbf{A}_{\tilde{R}\dot{e}}$ can be extracted as submatrices of \mathbf{A} .

Transfer eigenvalue problem (5.13). The transfer eigenvalue problem can be written in the following matrix form: Find $(\mathbf{v}, \lambda) \in \mathbb{R}^{N_{\partial\Omega_e}} \times \mathbb{R}^+$ such that

$$\mathbf{T}^T \mathbf{A}_{\dot{e}\dot{e}} \mathbf{T} \mathbf{v} = \lambda \frac{\alpha_{\min} h}{N_{\partial\Omega_e}} \mathbf{I}_{\partial\Omega_e} \mathbf{v},$$

where \mathbf{T} is the matrix corresponding to the transfer operator, $N_{\partial\Omega_e}$ is the number of FE nodes on $\partial\Omega_e$, and $\mathbf{I}_{\partial\Omega_e} \in \mathbb{R}^{N_{\partial\Omega_e} \times N_{\partial\Omega_e}}$ is the identity matrix on the degrees of freedom of $\partial\Omega_e$. Therefore, let $\hat{\mathbf{T}} = \begin{pmatrix} -\mathbf{A}_{\dot{\Omega}_e \dot{\Omega}_e}^{-1} \mathbf{A}_{\dot{\Omega}_e \partial\Omega_e} \\ \mathbf{I}_{\partial\Omega_e} \end{pmatrix}$, where $\dot{\Omega}_e$ and $\partial\Omega_e$ correspond to the interior nodes of Ω_e and the nodes on $\partial\Omega_e$, respectively, correspond to the energy-minimizing extension from $\partial\Omega_e$ to Ω_e ; cf. (3.12). Then $\mathbf{T} = \mathbf{R}_{\Omega_e \rightarrow \dot{e}} \hat{\mathbf{T}}$, where \dot{e} denotes the discrete interior of e . Again, all matrices involved in the transfer eigenvalue problem, $\mathbf{A}_{\dot{e}\dot{e}}$, $\mathbf{A}_{\dot{\Omega}_e \dot{\Omega}_e}$, and $\mathbf{A}_{\dot{\Omega}_e \partial\Omega_e}$, can be extracted from \mathbf{A} , and $\mathbf{R}_{\Omega_e \rightarrow \dot{e}}$ only requires the index sets of Ω_e and \dot{e} .

Remark 7.2. We can efficiently approximate the space spanned by the leading singular vectors of the transfer operator T by using randomization, as suggested in [9], in the context of localized model reduction. This is helpful since the transfer eigenvalue problem, which is defined on the nodes of $\partial\Omega_e$, may be significantly larger than the Dirichlet eigenvalue problem, which is defined on the interior nodes of e .

Orthogonalization of the edge functions. Let us remark that $V_{\Omega_e}^0|_e \cap V_{\Omega_e, \text{ha}}|_e \neq \emptyset$. Hence, even though the two spaces are a -orthogonal on Ω_e , when restricted to an edge, the functions from the two spaces may not be linearly independent anymore. In order to remove (almost) linearly dependent edge functions, we finally orthogonalize the edge functions for each edge using a proper orthogonal decomposition (POD) [8, 53].

Remark 7.3. The construction of our new algebraic adaptive coarse space requires additional algorithmic steps compared to nonalgebraic adaptive coarse spaces, such as [57, 18, 25], but those additional steps are local to Ω_e . After showing the feasibility of our new approach in this paper, we will further investigate potential improvements in terms of the complexity of the algorithm and its computational efficiency, for instance, using randomized linear algebra for solving the two eigenvalue problems.

8. Numerical results. In this section, we present numerical results demonstrating the robustness of our new adaptive coarse space introduced in (5.16). In particular, we consider model problem (2.1) with various heterogeneous coefficient functions on the computational domain $\Omega = [0, 1]^2$. We discretize using piecewise linear FEs on a regular mesh. Moreover, we use the preconditioned conjugate gradient (PCG) method and stop the iteration once $\|\mathbf{M}^{-1}r^{(k)}\|/\|\mathbf{M}^{-1}r^{(0)}\| < 10^{-10}$. The overlapping subdomains $\{\Omega_i\}_{i=1}^M$ are constructed algebraically, that is, by extending the nonoverlapping subdomains by one layer of FE nodes. In most of our numerical experiments, we start with nonoverlapping square subdomains, which also yields square overlapping subdomains. In the results in subsection 8.4, we additionally consider an unstructured nonoverlapping domain decomposition generated using METIS version 5.0 [33]. Moreover, we keep the tolerances for the selection of eigenfunctions in the Dirichlet eigenvalue problem $tol_{dir} = 10^{-3}$ and the tolerance for the POD orthogonalization $tol_o = 10^{-5}$ fixed. The tolerance for the transfer eigenvalue problem tol_{tr} is chosen as 10^5 in most cases and only varied in a few cases, as reported in the tables. The algorithms have been implemented and run using MATLAB_R2023a.

We compare the adaptive coarse space proposed in this paper in (5.16) and variants of it with the classical GDSW and AGDSW coarse spaces. Even though our theory holds for general coefficient functions, we are mostly interested in testing our coarse space for difficult configurations, where standard coarse spaces fail: We focus on discontinuous coefficient functions since they deteriorate convergence more than continuous coefficient functions; see also the results in subsection 8.4. Furthermore, it is well known that high-coefficient components fully contained inside the subdomains only have a minor influence on the convergence; see, for example, [19]. It has also been observed that examples where the high-coefficient components do not touch the Dirichlet boundary are more challenging; this is particularly evident for low numbers of subdomains. Therefore, except for the realistic coefficient function in subsection 8.4, we set a low coefficient on the elements which touch the boundary of the domain.

Additional results on the spectra of the eigenvalue problems as well as a comparison of the algebraic and nonalgebraic variants of the transfer eigenvalue problem are presented in section SM2.

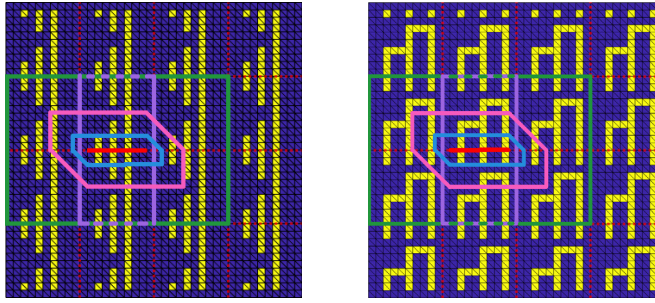


FIG. 4. Heterogeneous coefficient functions with high-coefficient channels of varying lengths (left) and comb-type components (right) cutting the interface of a 4×4 domain decomposition with $H/h = 10$. The interface is depicted as dashed red lines, elements with $\alpha = \alpha_{\max}$ are colored in yellow, and elements with $\alpha = \alpha_{\min}$ are colored in dark blue. Oversampling domains Ω_e of varying size are depicted: Ω_e^{2h} in light blue, Ω_e^{5h} in pink, Ω_e^H in light green, and the domain for the extensions in AGDSW eigenvalue problems in light purple; the discrete interior edge \hat{e} is plotted in solid red.

TABLE 1

Numerical results for the configuration shown in Figure 4 (left) with $\alpha_{\min} = 1, \alpha_{\max} = 10^6$; for the novel $X_{\text{VCD}}, X_{\text{VCT}},$ and X_{VCDT} coarse spaces, we vary the size of Ω_e . We report the coarse space dimensions (after/before proper orthogonal decomposition), estimated condition numbers, and iteration counts. Nondefault tol_{tr} is marked in boldface.

X_0	Ω_e	tol_{tr}	$\dim X_0$	κ	No. of iterations
X_{GDSW}	–	–	33/ 33	$2.7 \cdot 10^5$	118
X_{AGDSW}	–	–	57/ 57	7.4	24
X_{VCD}	Ω_e^{2h}	–	33/ 33	$2.7 \cdot 10^5$	118
	Ω_e^{5h}	–	57/ 57	7.2	24
	Ω_e^H	–	57/ 57	7.2	24
X_{VCT}	Ω_e^{2h}	10^5	93/105	7.6	24
	Ω_e^{5h}	10^5	57/ 66	19.0	36
	Ω_e^H	10^5	57/ 66	19.0	36
X_{VCDT}	Ω_e^{2h}	10^5	93/105	7.6	24
	Ω_e^{5h}	10^6	57/ 69	7.6	24
	Ω_e^H	10^5	57/ 90	7.2	25
			57/ 90	7.2	24

8.1. A first model problem: Channels of varying lengths. As a first model problem, we consider the coefficient function shown in Figure 4 (left). The results are listed in Table 1, where, here and elsewhere, the reported condition number is estimated from the Lanczos process within PCG. The results clearly show the bad performance of the classical GDSW coarse space; in fact, the condition number of $2.7 \cdot 10^5$ is close to the contrast $\alpha_{\max}/\alpha_{\min} = 10^6$ itself. Due to the moderate number of subdomains, the resulting iteration count is still moderate, that is, 118. Both the AGDSW and the new coarse space yield a low condition number below 10 and fast convergence within 24 or 25 iterations.

In Table 1, we also provide results for only using one of the two eigenvalue problems, that is, either only the Dirichlet eigenvalue problem (X_{VCD}) or only the transfer eigenvalue problem (X_{VCT}). We observe that, once Ω_e gets too small (Ω_e^{2h}), the Dirichlet eigenvalue problem fails to detect the high-coefficient channels. The resulting coarse space just corresponds to the standard GDSW coarse space. On the other hand, for this example, the transfer eigenvalue problem alone already yields a robust

TABLE 2

Numerical results for the configuration shown in Figure 4 (left) with varying α_{\min} and $\alpha_{\max} = 10^6$ using the classical X_{GDSW} and adaptive X_{VCDT} ($\Omega_e = \Omega_e^{5h}$) coarse spaces. We report the coarse space dimensions (after/before POD), estimated condition numbers, and iteration counts.

α_{\min}	X_0	tol_{tr}	$\dim X_0$	κ	No. of iterations
10^{-2}	X_{GDSW}	–	33/33	$2.7 \cdot 10^7$	142
	X_{VCDT}	10^4	57/93	7.3	25
1	X_{GDSW}	–	33/33	$2.7 \cdot 10^5$	118
	X_{VCDT}	10^4	57/93	7.2	25
10^2	X_{GDSW}	–	33/33	$2.7 \cdot 10^3$	95
	X_{VCDT}	10^4	57/69	8.5	25

coarse space. However, for Ω_e^{2h} , the transfer eigenvalue problem yields unnecessary eigenmodes for the default tolerance 10^5 . Table 1 shows that, when increasing the tolerance to 10^6 , those unnecessary eigenmodes are omitted; see also subsection SM2.1.

Furthermore, we observe that there is a significant amount of linearly dependent edge basis functions for the new coarse space; this results from the fact that we combine the constant function and eigenfunctions from the Dirichlet and transfer eigenvalue problem. Due to POD orthogonalization, the total coarse space dimension is reduced by 12–15. Here, the resulting coarse space dimension of 57 is always optimal, which can be explained as follows: For each edge, we need at least one (constant) function and, in case of channels cutting the edge, at least as many functions as channels. This yields $12 + 3 \times 12 = 48$ edge functions. In addition to that, we obtain one function for each of the nine vertices, resulting in a dimension of 57.

Finally, we report results for varying values of α_{\min} in Table 2 to investigate the robustness with respect to the contrast of the coefficient. We observe that the classical GDSW coarse space is not robust with respect to the coefficient contrast: The condition number is in the order of the coefficient contrast, and the convergence deteriorates with decreasing values of α_{\min} . For the X_{VCDT} coarse space, the results are robust and independent of α_{\min} .

8.2. Dimension reduction of the coarse space by enlarging Ω_e . In subsection 8.1, we already observed the influence of the size of Ω_e on the spectra of the eigenvalue problems. Here, we discuss a second example, which is visualized in Figure 4 (right), where the effect is even stronger and better interpretable.

It can be observed that a single edge function, yielding a coarse space of dimension 33, is sufficient for robustness for this example because there is only a single connected high-coefficient component cutting each edge. Consequently, in Table 3, even the classical GDSW coarse yields good results. This can only be detected by the eigenvalue problem if Ω_e is large enough to cover this whole high-coefficient component (Ω_e^H). If Ω_e is too small, then the high-coefficient component may appear as either two or three components cutting the edge for Ω_e^{2h} or Ω_e^{5h} , respectively; cf. Figure 4 (right). Also, when using the two subdomains adjacent to the edge e for the energy-minimizing extension, as in the AGDSW approach, the component is detected as a whole.

This is also reflected clearly in the numerical results in Table 3. There are 12 edges cut by such a high-coefficient component. While increasing the size of Ω_e from Ω_e^{2h} to Ω_e^{5h} or Ω_e^H , the coarse space dimension reduces by 12 or 24, respectively. The same behavior can be observed for AGDSW when using Ω_e^{2h} , Ω_e^{5h} , and Ω_e^H as the extension domain. This effect has already been reported for similar cases in [26].

TABLE 3

Numerical results for the configuration shown in Figure 4 (right) with $\alpha_{\min} = 1, \alpha_{\max} = 10^6$; for the X_{GDSW} and the novel X_{VCDT} coarse spaces, we vary the size of Ω_e . We report the coarse space dimensions (after/before POD), estimated condition numbers, and iteration counts. Nondefault tol_{tr} is marked in boldface.

X_0	Ω_e	tol_{tr}	$\dim X_0$	κ	No. of iterations
X_{GDSW}	–	–	33/33	24.1	31
X_{AGDSW}	Ω_e^{2h}	–	57/57	7.1	24
	Ω_e^{5h}	–	45/45	12.6	26
	Ω_e^H	–	33/33	24.1	31
	–	–	33/33	24.1	31
X_{VCDT}	Ω_e^{2h}	10^6	57/69	7.1	24
	Ω_e^{5h}	10^5	45/57	17.1	33
	Ω_e^H	10^5	33/57	24.1	31

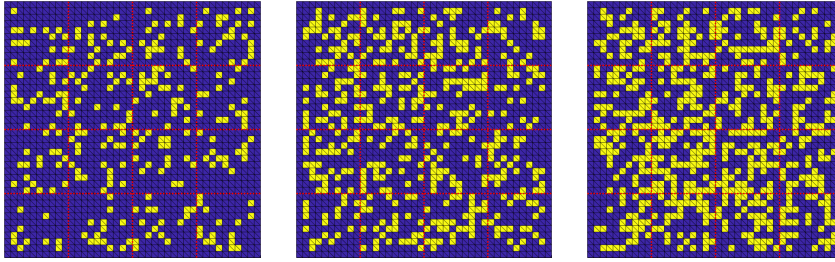


FIG. 5. Exemplary random heterogeneous coefficient functions with 20% (left), 30% (middle), and 40% (right) elements with high coefficients on a 4×4 domain decomposition with $H/h = 10$. The interface is depicted as dashed red lines, the elements with $\alpha = \alpha_{\max}$ are colored in yellow, and the elements with $\alpha = \alpha_{\min}$ are colored in dark blue.

8.3. Random coefficient distributions. In order to validate the theory and show robustness of our new algebraic approach (X_{VCDT} coarse space) for general coefficient distributions, we test it on randomly distributed binary coefficient distributions; examples for coefficient distributions with 20%, 30%, and 40% elements with high coefficients are shown in Figure 5.

The results are listed in Table 4, and we can draw several conclusions from those results. First, we generally obtain good convergence for our new algebraic approach for different ratios of high-coefficient elements and sizes of Ω_e . As we already observed before, enlarging Ω_e reduces the coarse space dimension, which is much more pronounced for larger ratios of high-coefficient elements; for instance, for 40% of high-coefficient elements, the coarse space dimension can be reduced from 155.1 to 59.0 on average when keeping the tolerances fixed.

Of course, enlarging Ω_e also increases the computational work for setting up both eigenvalue problems. As an alternative, we consider the smallest $\Omega_e = \Omega_e^{2h}$ and vary the tolerance for the transfer eigenvalue problem for the tolerance: When increasing tol_{tr} from 10^4 to 10^6 , the coarse space dimension reduces from 162.3 to 119.0. At the same time, the condition number and iteration count increase moderately: The maximum iteration count goes up from 34 to 44 and the maximum condition number from 29.4 to 1879.4. When increasing the tolerance further to 10^7 , we obtain an even smaller coarse space dimension of 79.9; however, the maximum condition number and iteration count deteriorate to $9.6 \cdot 10^4$ and 105, respectively. Obtaining robustness

TABLE 4

Numerical results for the configurations shown in Figure 5 with randomly distributed coefficient functions and $\alpha_{\min} = 1, \alpha_{\max} = 10^6$ using the novel X_{VCDT} coarse space using varying sizes of Ω_e . We report the coarse space dimensions (after/before POD), estimated condition numbers, and iteration counts averaged over 100 runs (maximum in parentheses). Nondefault tol_{tr} are marked in boldface.

α_{\max}	Ω_e	tol_{tr}	dim X_0	κ	No. of iterations
20 %	Ω_e^{2h}	10^5	85.7(105)/128.5(150)	12.1 (36.0)	30.1 (36)
	Ω_e^{5h}	10^5	62.6(77)/127.3(158)	9.1 (27.9)	27.8 (32)
	Ω_e^H	10^5	62.4(74)/122.3(142)	8.6 (11.6)	27.5 (31)
30 %	Ω_e^{2h}	10^5	121.6(143)/154.8(176)	20.6 (86.3)	30.0 (41)
	Ω_e^{5h}	10^5	70.6(81)/122.7(143)	10.6 (25.5)	27.4 (34)
	Ω_e^H	10^5	62.9(74)/122.4(143)	13.3 (38.4)	27.6 (37)
40 %	Ω_e^{2h}	10^7	79.9(87)/ 81.2(88)	$1.1 \cdot 10^4$ ($9.6 \cdot 10^4$)	51.4 (105)
		10^6	119.0(133)/125.5(136)	223.9 (1879.4)	34.6 (59)
		10^5	155.1(172)/180.7(200)	17.2 (296.0)	25.5 (33)
		10^4	162.3(179)/190.9(210)	6.7 (29.4)	21.7 (26)
	Ω_e^{5h}	10^5	81.3(94)/112.3(126)	11.5 (40.6)	27.3 (34)
		10^5	59.0(68)/ 95.2(116)	23.3 (76.9)	32.9 (44)

using the algebraic coarse space depends on an interplay of the hyperparameters of the method, such as the size of Ω_e and the tolerances.

8.4. Modified SPE10 model problem. Finally, we consider a coefficient function based on realistic data. In particular, we use heterogeneous coefficient functions α generated from parts of the 40th layer of the second data set from the 2001 SPE Comparative Solution Project benchmark [12], employing the pixelwise norm of the permeabilities as the coefficient function. Notably, this example can be solved robustly using the classical GDSW coarse space, and no adaptive coarse space is needed. However, if we convert α into a binary coefficient function by setting all coefficients above 1.0 to $\alpha_{\max} = 10^6$ and all coefficients below 1.0 to $\alpha_{\min} = 1$, then the classical GDSW coarse space is not robust anymore, resulting in a high condition number of $2.0 \cdot 10^5$. Note that we chose one of the more difficult layers; other layers tested exemplarily were less challenging for the preconditioners considered. Here, in addition to square subdomains, we also consider an unstructured domain decomposition into 25 subdomains generated by METIS.

As can be seen from Table 5, for the square subdomains, as expected, the X_{AGDSW} and X_{VCDT} adaptive coarse spaces yield robust results. For small sizes of Ω_e , the dimension of the X_{VCDT} coarse space is quite high; for instance, the coarse space dimension is 362 for $\Omega_e = \Omega_e^{2h}$ (and $tol_{tr} = 10^5$). We observe that the coarse space dimension reduces significantly when increasing tol_{tr} ; for $tol_{tr} = 10^7$, the dimension is only 147. The same dimension is obtained for $\Omega_e = \Omega_e^H$. While enlarging Ω_e results in a better condition number and iteration count, it also increases the computational cost of the eigenvalue problems. On the other hand, increasing tol_{tr} does not increase the computational cost; however, the condition number and iteration count grow moderately.

We also report results for the space X_{VCD} , where the transfer eigenvalue problem is completely neglected. While the condition number is contrast dependent for $\Omega_e = \Omega_e^{2h}$, which shows that the transfer eigenvalue problem is necessary in this case, we obtain good results for $\Omega_e = \Omega_e^{5h}$ and $\Omega_e = \Omega_e^H$; notably, the dimension of X_{VCD} is even lower than that of X_{AGDSW} . Note that if the oversampling domain is mostly

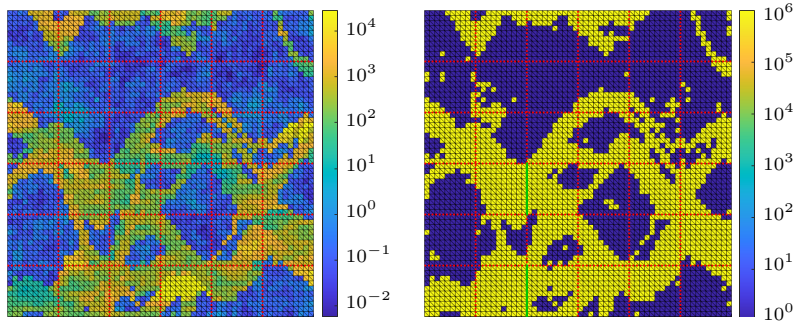


FIG. 6. SPE10 coefficient functions on a 6×6 domain decomposition with $H/h = 10$; the interface is depicted as dashed red lines. Top: Permeability distribution. Right: Binary distribution using a threshold of 1: Values ≥ 1 are mapped to $\alpha_{\max} = 10^6$ and values < 1 to $\alpha_{\min} = 1$.

TABLE 5

Numerical results for the configurations shown in Figure 6; for the novel X_{VCD} and X_{VCDT} coarse space, we vary the size of Ω_e . We report the coarse space dimensions (after/before POD), estimated condition numbers, and iteration counts. Nondefault tol_{tr} are marked in boldface.

X_0	Ω_e	tol_{tr}	Structured DD			METIS DD		
			dim X_0	κ	# its.	dim X_0	κ	No. of iterations
Original coefficient (without thresholding)								
X_{GDSW}	–	–	85/ 85	20.6	42	88/ 88	24.4	39
Binary coefficient (with thresholding)								
X_{GDSW}	–	–	85/ 85	$2.0 \cdot 10^5$	57	88/ 88	$3.2 \cdot 10^5$	54
X_{AGDSW}	–	–	93/ 93	19.3	38	96/ 96	16.2	36
	Ω_e^{2h}	10^7	147/150	1859.0	40	160/161	$9.1 \cdot 10^4$	43
		10^6	262/273	122.8	37	265/277	522.6	36
	X_{VCDT}	10^5	362/417	9.3	31	303/345	9.9	30
	Ω_e^{5h}	10^5	191/229	9.3	31	193/222	8.5	29
	Ω_e^H	10^5	147/176	9.6	31	157/192	14.2	31
X_{VCD}	Ω_e^{2h}	–	87/ 89	$2.0 \cdot 10^5$	57	88/ 88	$3.2 \cdot 10^5$	54
	Ω_e^{5h}	–	90/ 92	19.4	39	94/ 96	16.5	37
	Ω_e^H	–	90/ 93	19.4	39	94/ 97	16.5	36

covered by high-coefficient elements, then we conjecture a slower decay of the harmonic extensions of higher-frequency modes on $\partial\Omega_e$. This results in a relatively large X_{VCT} space on e ; this is the case, for example, for the green vertical edges in Figure 6.

The results for the METIS DD are consistent with the results obtained for the square subdomains. We observe that even though the number of subdomains is lower than for the structured case—25 instead of 36—the number of interface components is slightly higher: We obtain 56 instead of 60 edges and 32 instead of 25 vertices, respectively. Correspondingly, we obtain larger coarse spaces for unstructured domain decompositions, which is a typical observation for interface-based coarse spaces.

These results show that our algebraic approach is very robust, but further investigations of choosing the tolerances will be necessary to obtain the optimal coarse space dimension. This is a common challenge in adaptive coarse spaces; see, for instance, the discussion in [28]. A full investigation will be the subject of future research.

REFERENCES

- [1] E. AGULLO, L. GIRAUD, AND L. POIREL, *Robust preconditioners via generalized eigenproblems for hybrid sparse linear solvers*, SIAM J. Matrix Anal. Appl., 40 (2019), pp. 417–439, <https://doi.org/10.1137/17M1153765>.
- [2] H. AL DAAS AND L. GRIGORI, *A class of efficient locally constructed preconditioners based on coarse spaces*, SIAM J. Matrix Anal. Appl., 40 (2019), pp. 66–91, <https://doi.org/10.1137/18M1194365>.
- [3] H. AL DAAS AND P. JOLIVET, *A robust algebraic multilevel domain decomposition preconditioner for sparse symmetric positive definite matrices*, SIAM J. Sci. Comput., 44 (2022), pp. A2582–A2598, <https://doi.org/10.1137/21M1446320>.
- [4] H. AL DAAS, P. JOLIVET, AND T. REES, *Efficient algebraic two-level Schwarz preconditioner for sparse matrices*, SIAM J. Sci. Comput., 45 (2023), pp. A1199–A1213, <https://doi.org/10.1137/22M1469833>.
- [5] I. BABUŠKA AND R. LIPTON, *Optimal local approximation spaces for generalized finite element methods with application to multiscale problems*, Multiscale Model. Simul., 9 (2011), pp. 373–406, <https://doi.org/10.1137/100791051>.
- [6] P. BASTIAN, R. SCHEICHL, L. SEELINGER, AND A. STREHLow, *Multilevel spectral domain decomposition*, SIAM J. Sci. Comput., 45 (2023), pp. S1–S26, <https://doi.org/10.1137/21M1427231>.
- [7] L. BERGER-VERGIAT, C. A. GLUSA, J. J. HU, M. MAYR, A. PROKOPENKO, C. M. SIEFERT, R. S. TUMINARO, AND T. A. WIESNER, *MueLu User's Guide*, Technical report SAND2019-0537, Sandia National Laboratories, 2019.
- [8] G. BERKOOZ, P. HOLMES, AND J. L. LUMLEY, *The proper orthogonal decomposition in the analysis of turbulent flows*, Annu. Rev. Fluid Mech., 25 (1993), pp. 539–575, <https://doi.org/10.1146/annurev.fl.25.010193.002543>.
- [9] A. BUHR AND K. SMETANA, *Randomized local model order reduction*, SIAM J. Sci. Comput., 40 (2018), pp. A2120–A2151, <https://doi.org/10.1137/17M1138480>.
- [10] J. G. CALVO AND O. B. WIDLUND, *An adaptive choice of primal constraints for BDDC domain decomposition algorithms*, Electron. Trans. Numer. Anal., 45 (2016), pp. 524–544, <https://etna.math.kent.edu/volumes/2011-2020/vol45/abstract.php?vol=45&pages=524-544>.
- [11] T. CHARTIER, R. D. FALGOUT, V. E. HENSON, J. JONES, T. MANTEUFFEL, S. MCCORMICK, J. RUGE, AND P. S. VASSILEVSKI, *Spectral AMGe (ρ AMGe)*, SIAM J. Sci. Comput., 25 (2003), pp. 1–26, <https://doi.org/10.1137/S106482750139892X>.
- [12] M. A. CHRISTIE AND M. BLUNT, *Tenth SPE comparative solution project: A comparison of up-scaling techniques*, SPE Reserv. Eval. Eng., 4 (2001), pp. 308–317, <https://doi.org/10.2118/72469-PA>.
- [13] C. R. DOHRMANN, A. KLAWONN, AND O. B. WIDLUND, *Domain decomposition for less regular subdomains: Overlapping Schwarz in two dimensions*, SIAM J. Numer. Anal., 46 (2008), pp. 2153–2168, <https://doi.org/10.1137/070685841>.
- [14] C. R. DOHRMANN, A. KLAWONN, AND O. B. WIDLUND, *A family of energy minimizing coarse spaces for overlapping Schwarz preconditioners*, in Domain Decomposition Methods in Science and Engineering XVII, Springer-Verlag, Berlin, 2008, pp. 247–254.
- [15] V. DOLEAN, F. NATAF, R. SCHEICHL, AND N. SPILLANE, *Analysis of a two-level Schwarz method with coarse spaces based on local Dirichlet-to-Neumann maps*, Comput. Methods Appl. Math., 12 (2012), pp. 391–414, <https://doi.org/10.2478/cmam-2012-0027>.
- [16] M. DRYJA AND O. B. WIDLUND, *Domain decomposition algorithms with small overlap*, SIAM J. Sci. Comput., 15 (1994), pp. 604–620, <https://doi.org/10.1137/0915040>.
- [17] J. GALVIS AND Y. EFENDIEV, *Domain decomposition preconditioners for multiscale flows in high-contrast media*, Multiscale Model. Simul., 8 (2010), pp. 1461–1483, <https://doi.org/10.1137/090751190>.
- [18] M. J. GANDER, A. LONELAND, AND T. RAHMAN, *Analysis of a New Harmonically Enriched Multiscale Coarse Space for Domain Decomposition Methods*, preprint, arXiv:1512.05285, 2015.
- [19] S. GIPPERT, A. KLAWONN, AND O. RHEINBACH, *Analysis of FETI-DP and BDDC for linear elasticity in 3D with almost incompressible components and varying coefficients inside subdomains*, SIAM J. Numer. Anal., 50 (2012), pp. 2208–2236, <https://doi.org/10.1137/110838315>.
- [20] G. H. GOLUB AND C. F. VAN LOAN, *Matrix Computations*, 4th ed., The Johns Hopkins University Press, Baltimore, MD, 2013.

- [21] L. GOUARIN AND N. SPILLANE, *Fully algebraic domain decomposition preconditioners with adaptive spectral bounds*, Electron. Trans. Numer. Anal., 60 (2024), pp. 169–196, <https://etna.math.kent.edu/vol.60.2024/pp169-196.dir/pp169-196.pdf>.
- [22] I. GRAHAM, P. LECHNER, AND R. SCHEICHL, *Domain decomposition for multiscale PDEs*, Numer. Math., 106 (2007), pp. 589–626, <https://doi.org/10.1007/s00211-007-0074-1>.
- [23] A. HEINLEIN, *Parallel Overlapping Schwarz Preconditioners and Multiscale Discretizations with Applications to Fluid-Structure Interaction and Highly Heterogeneous Problems*, Ph.D. thesis, University of Cologne, Cologne, Germany, 2016.
- [24] A. HEINLEIN, C. HOCHMUTH, AND A. KLAWONN, *Fully algebraic two-level overlapping Schwarz preconditioners for elasticity problems*, in Numerical Mathematics and Advanced Applications—ENUMATH 2019, Lecture Notes in Computational Science and Engineering 139, Springer-Verlag, Berlin, 2021, pp. 531–539.
- [25] A. HEINLEIN, A. KLAWONN, J. KNEPPER, AND O. RHEINBACH, *Multiscale coarse spaces for overlapping Schwarz methods based on the ACMS space in 2D*, Electron. Trans. Numer. Anal., 48 (2018), pp. 156–182, https://doi.org/10.1553/etna_vol48s156.
- [26] A. HEINLEIN, A. KLAWONN, J. KNEPPER, AND O. RHEINBACH, *Adaptive GDSW coarse spaces for overlapping Schwarz methods in three dimensions*, SIAM J. Sci. Comput., 41 (2019), pp. A3045–A3072, <https://doi.org/10.1137/18M1220613>.
- [27] A. HEINLEIN, A. KLAWONN, J. KNEPPER, O. RHEINBACH, AND O. B. WIDLUND, *Adaptive GDSW coarse spaces of reduced dimension for overlapping Schwarz methods*, SIAM J. Sci. Comput., 44 (2022), pp. A1176–A1204, <https://doi.org/10.1137/20M1364540>.
- [28] A. HEINLEIN, A. KLAWONN, AND M. KÜHN, *Local spectra of adaptive domain decomposition methods*, in International Conference on Domain Decomposition Methods, Springer-Verlag, Berlin, 2018, pp. 167–175.
- [29] A. HEINLEIN, A. KLAWONN, M. LANSER, AND J. WEBER, *A frugal FETI-DP and BDDC coarse space for heterogeneous problems*, Electron. Trans. Numer. Anal., 53 (2020), pp. 562–591, https://doi.org/10.1553/etna_vol53s562.
- [30] A. HEINLEIN, A. KLAWONN, S. RAJAMANICKAM, AND O. RHEINBACH, *FROSch: A fast and robust overlapping Schwarz domain decomposition preconditioner based on Xpetra in Trilinos*, in Domain Decomposition Methods in Science and Engineering XXV, Lecture Notes in Computational Science and Engineering 138, Springer-Verlag, Berlin, 2020, pp. 176–184, https://link.springer.com/chapter/10.1007/978-3-030-56750-7_19.
- [31] A. HEINLEIN, A. KLAWONN, AND O. RHEINBACH, *A parallel implementation of a two-level overlapping Schwarz method with energy-minimizing coarse space based on Trilinos*, SIAM J. Sci. Comput., 38 (2016), pp. C713–C747, <https://doi.org/10.1137/16M1062843>.
- [32] M. A. HEROUX, R. A. BARTLETT, V. E. HOWLE, R. J. HOEKSTRA, J. J. HU, T. G. KOLDA, R. B. LEHOUCQ, K. R. LONG, R. P. PAWLOWSKI, E. T. PHIPPS, A. G. SALINGER, H. K. THORNQUIST, R. S. TUMINARO, J. M. WILLENBRING, A. WILLIAMS, AND K. S. STANLEY, *An overview of the Trilinos Project*, ACM Trans. Math. Software, 31 (2005), pp. 397–423, <https://doi.org/10.1145/1089014.1089021>.
- [33] G. KARYPIS AND V. KUMAR, *METIS: A Software Package for Partitioning Unstructured Graphs, Partitioning Meshes, and Computing Fill-Reducing Orderings of Sparse Matrices*, Technical report 97-061, University of Minnesota, Minneapolis, 1997, <https://hdl.handle.net/11299/215346>.
- [34] G. KARYPIS AND V. KUMAR, *A fast and high quality multilevel scheme for partitioning irregular graphs*, SIAM J. Sci. Comput., 20 (1998), pp. 359–392, <https://doi.org/10.1137/S1064827595287997>.
- [35] H. H. KIM, E. CHUNG, AND J. WANG, *BDDC and FETI-DP preconditioners with adaptive coarse spaces for three-dimensional elliptic problems with oscillatory and high contrast coefficients*, J. Comput. Phys., 349 (2017), pp. 191–214, <https://doi.org/10.1016/j.jcp.2017.08.003>.
- [36] A. KLAWONN, M. KÜHN, AND O. RHEINBACH, *Adaptive coarse spaces for FETI-DP in three dimensions*, SIAM J. Sci. Comput., 38 (2016), pp. A2880–A2911, <https://doi.org/10.1137/15M1049610>.
- [37] A. KLAWONN, P. RADTKE, AND O. RHEINBACH, *FETI-DP methods with an adaptive coarse space*, SIAM J. Numer. Anal., 53 (2015), pp. 297–320, <https://doi.org/10.1137/130939675>.
- [38] J. KNEPPER, *Adaptive Coarse Spaces for the Overlapping Schwarz Method and Multiscale Elliptic Problems*, Ph.D. thesis, University of Cologne, Cologne, Germany, 2022.
- [39] R. KORNUBER, D. PETERSEIM, AND H. YSERENTANT, *An analysis of a class of variational multiscale methods based on subspace decomposition*, Math. Comp., 87 (2018), pp. 2765–2774, <https://doi.org/10.1090/mcom/3302>.

- [40] R. KORNUBER AND H. YSERENTANT, *Numerical homogenization of elliptic multiscale problems by subspace decomposition*, *Multiscale Model. Simul.*, 14 (2016), pp. 1017–1036, <https://doi.org/10.1137/15M1028510>.
- [41] C. MA, R. SCHEICHL, AND T. DODWELL, *Novel design and analysis of generalized finite element methods based on locally optimal spectral approximations*, *SIAM J. Numer. Anal.*, 60 (2022), pp. 244–273, <https://doi.org/10.1137/21M1406179>.
- [42] A. MÅLQVIST AND D. PETERSEIM, *Localization of elliptic multiscale problems*, *Math. Comp.*, 83 (2014), pp. 2583–2603, <https://doi.org/10.1090/S0025-5718-2014-02868-8>.
- [43] J. MANDEL AND B. SOUSEDÍK, *Adaptive selection of face coarse degrees of freedom in the BDDC and the FETI-DP iterative substructuring methods*, *Comput. Methods Appl. Mech. Engrg.*, 196 (2007), pp. 1389–1399, <https://doi.org/10.1016/j.cma.2006.03.010>.
- [44] H. OWHADI, *Multigrid with rough coefficients and multiresolution operator decomposition from hierarchical information games*, *SIAM Rev.*, 59 (2017), pp. 99–149, <https://doi.org/10.1137/15M1013894>.
- [45] H. OWHADI AND L. ZHANG, *Localized bases for finite-dimensional homogenization approximations with nonseparated scales and high contrast*, *Multiscale Model. Simul.*, 9 (2011), pp. 1373–1398, <https://doi.org/10.1137/100813968>.
- [46] H. OWHADI, L. ZHANG, AND L. BERLYAND, *Polyharmonic homogenization, rough polyharmonic splines and sparse super-localization*, *ESAIM Math. Model. Numer. Anal.*, 48 (2014), pp. 517–552, <https://doi.org/10.1051/m2an/2013118>.
- [47] C. PECHSTEIN AND C. R. DOHRMANN, *A unified framework for adaptive BDDC*, *Electron. Trans. Numer. Anal.*, 46 (2017), pp. 273–336, <https://etna.math.kent.edu/volumes/2011-2020/vol46/abstract.php?vol=46&pages=273-336>.
- [48] A. PINKUS, *n-Widths in Approximation Theory*, *Ergeb. Math. Grenzgeb. (3)* 7, Springer-Verlag, Berlin, 1985.
- [49] A. QUARTERONI AND A. VALLI, *Domain Decomposition Methods for Partial Differential Equations*, *Numerical Mathematics and Scientific Computation*, Clarendon Press, Oxford, 1999.
- [50] J. W. RUGE AND K. STÜBEN, *Algebraic multigrid*, in *Multigrid Methods*, SIAM, Philadelphia, 1987, pp. 73–130.
- [51] J. SCHLEUSS AND K. SMETANA, *Optimal local approximation spaces for parabolic problems*, *Multiscale Model. Simul.*, 20 (2022), pp. 551–582, <https://doi.org/10.1137/20M1384294>.
- [52] J. SCHLEUSS, K. SMETANA, AND L. TER MAAT, *Randomized quasi-optimal local approximation spaces in time*, *SIAM J. Sci. Comput.*, 45 (2023), pp. A1066–A1096, <https://doi.org/10.1137/22M1481002>.
- [53] L. SIROVICH, *Turbulence and the dynamics of coherent structures. I. Coherent structures*, *Quart. Appl. Math.*, 45 (1987), pp. 561–571, <https://doi.org/10.1090/qam/910462>.
- [54] K. SMETANA AND A. T. PATERA, *Optimal local approximation spaces for component-based static condensation procedures*, *SIAM J. Sci. Comput.*, 38 (2016), pp. A3318–A3356, <https://doi.org/10.1137/15M1009603>.
- [55] N. SPILLANE, *An Abstract Theory of Domain Decomposition Methods with Coarse Spaces of the GenEO Family*, preprint, arXiv:2104.00280, 2021.
- [56] N. SPILLANE, *Toward a new fully algebraic preconditioner for symmetric positive definite problems*, in *Domain Decomposition Methods in Science and Engineering XXVI*, Springer-Verlag, Berlin, 2023, pp. 745–752.
- [57] N. SPILLANE, V. DOLEAN, P. HAURET, F. NATAF, C. PECHSTEIN, AND R. SCHEICHL, *Abstract robust coarse spaces for systems of PDEs via generalized eigenproblems in the overlaps*, *Numer. Math.*, 126 (2014), pp. 741–770, <https://doi.org/10.1007/s00211-013-0576-y>.
- [58] N. SPILLANE AND D. J. RIXEN, *Automatic spectral coarse spaces for robust finite element tearing and interconnecting and balanced domain decomposition algorithms*, *Internat. J. Numer. Methods Engrg.*, 95 (2013), pp. 953–990, <https://doi.org/10.1002/nme.4534>.
- [59] A. TOSELLI AND O. WIDLUND, *Domain Decomposition Methods—Algorithms and Theory*, *Springer Series in Computational Mathematics* 34, Springer-Verlag, Berlin, 2005.